Remote Sensing of Environment 138 (2013) 102–118

Contents lists available at ScienceDirect

Remote Sensing of Environment

journal homepage: www.elsevier.com/locate/rse

Temporal upscaling of instantaneous evapotranspiration: An intercomparison of four methods using eddy covariance measurements and MODIS data

Ronglin Tang [a], Zhao-Liang Li [b,c,*], Xiaomin Sun [d]

[a] State Key Laboratory of Resources and Environment Information System, Institute of Geographic Sciences and Natural Resources Research, Beijing 100101, China
[b] Key Laboratory of Agri-informatics, Ministry of Agriculture/Institute of Agricultural Resources and Regional Planning, Chinese Academy of Agricultural Sciences, Beijing 100081, China
[c] ICube, UdS, CNRS, Bld Sebastien Brant, BP10413, 67412 Illkirch, France
[d] Key Laboratory of Ecosystem Network Observation and Modeling, Institute of Geographic Sciences and Natural Resources Research, Beijing 100101, China

ARTICLE INFO

Article history:
Received 14 December 2012
Received in revised form 26 April 2013
Accepted 6 July 2013
Available online 15 August 2013

Keywords:
Evapotranspiration
Temporal upscaling
Eddy covariance system
MODIS

ABSTRACT

The quantification of land surface evapotranspiration (ET) at daily or longer time scales is of great significance in modeling the global hydrological cycle, studying climate change, and managing water resources. However, current remote sensing-based ET models can generally only provide snapshots of ET at the time of a satellite overpass and do not satisfy the expectations of hydrologists, irrigation engineers, or water resource managers concerned with practical applications. Four commonly used ET upscaling schemes, namely, the constant reference evaporative fraction (EF_r) method, the constant evaporative fraction (EF) method, the constant extraterrestrial solar radiation ratio (R_p) method, and the constant observed global solar radiation ratio (R_g) method, were evaluated in this study using ground-based eddy covariance (EC) measurements and the Moderate Resolution Imaging Spectroradiometer (MODIS) derived estimates from a two-source energy balance model. Analysis was made of both closed and un-closed surface fluxes and of different assumed satellite overpass times from mid-morning to mid-afternoon. Data for the analysis were collected at the Yucheng comprehensive experimental station in Northern China, spanning the period from late April 2009 to late October 2011. The results show that all four upscaling factors from noon to mid-afternoon had a better agreement with their corresponding daily averages. Overall, the EF_r (R_g) method had the best (second best) performance of the four upscaling methods. The EF method was found to significantly underestimate the daily latent heat flux (LE) and performed the worst of the four upscaling methods. With the correction of the energy imbalance of EC measurements, the R_g method's performance was improved and outperformed the EF_r method in the morning. The presence of clouds either increased or decreased the BIAS but generally increased the root mean square error (RMSE) for all four upscaling methods. When the upscaling methods were applied to convert the instantaneous MODIS remote sensing estimates of ET to daily values, the accuracy of the extrapolated daily ET was controlled by the accuracy of both the remote sensing ET estimates and the upscaling methods themselves. With the insignificantly biased estimates of the instantaneous LE from the N95 model at 101 MODIS overpass times in this study, using the EF method underestimated the daily ET by 11%, while all the remaining three factors overestimated the daily ET by a range of 5%–18%. This study was conducted to provide a scientific basis for developing an operational and more accurate ET-upscaling method with easy access to data in future studies.

1. Introduction

The estimation of surface evapotranspiration (ET, water in mm equivalent to latent heat flux) is of critical significance in global hydrological cycle modeling, climate change investigations, water resources planning and management, and the numerical modeling of weather forecasts. A number of ground-based networks have been established worldwide over the past few decades to monitor the long-term surface water, heat, and momentum transfer across different plant functional types (Baldocchi et al., 2001). However, these measurements are essentially point-scale data due to their limited spatial representativeness, and they cannot be spatially extrapolated over the large, heterogeneous surface of the Earth. Remote sensing technology provides the possibility of mapping the surface ET at different spatial scales, and various ET models based on remote sensing data have been developed with different degrees of complexity (see the latest overviews by Kalma, McVicar, and McCabe (2008) and Li et al. (2009)). Nevertheless, these ET models can generally only provide snapshots of ET at the time of a satellite overpass and do not satisfy the expectations of

* Corresponding author at: Key Laboratory of Agri-informatics, Ministry of Agriculture/Institute of Agricultural Resources and Regional Planning, Chinese Academy of Agricultural Sciences, Beijing 100081, China. Tel.: +86 10 82105077.
E-mail address: lizhaoliang@caas.cn (Z.-L. Li).

0034-4257/$ – see front matter © 2013 Elsevier Inc. All rights reserved.
http://dx.doi.org/10.1016/j.rse.2013.07.001

hydrologists, irrigation engineers, or water resource managers concerned with practical applications. It is therefore imperative to develop effective methods to temporally upscale the instantaneous ET to daily or longer integrated values of interest. The key to the development of various ET upscaling methods is to relate the targeted longer time-scale ET to a factor that can be nearly constant during the daytime or throughout a diurnal cycle.

One of the most commonly used approaches in converting instantaneous ET to daily values is the well-known constant evaporative fraction (EF) method (Shuttleworth, Gurney, Hsu, & Ormsby, 1989), in which EF is defined as the ratio of latent heat flux (LE, used interchangeably with ET in this paper) to surface available energy (surface net radiation minus soil heat flux). This method explicitly assumes the relative conservation of EF during the daytime, and its effectiveness in upscaling remote sensing estimates of instantaneous ET has been demonstrated by a variety of studies (Brutsaert & Sugita, 1992; Nichols & Cuenca, 1993; Crago, 1996; Lhomme & Elguero, 1999; Gentine, Entekhabi, Chehbouni, Boulet, & Duchemin, 2007). Once the daytime integrated surface available energy and the instantaneous EF at the satellite overpass time are derived, the daytime ET can be estimated by definition using the EF conservation method. Note that because the EF is controlled by both environmental factors and surface wetness conditions, several studies have reported that the EF curve exhibits a concave shape under wet conditions during the daytime on clear-sky or constant-cloud days (Lhomme & Elguero, 1999; Hoedjes, Chehbouni, Jacob, Ezzahar, & Boulet, 2008) and that its conservation can be jeopardized by intermittent clouds and horizontal advection. Furthermore, Gentine et al. (2007) concluded, based on simulations with a two-source soil–vegetation–atmosphere transfer model forced by the long-term SUDMED project data, that the degree to which the daytime EF is self-conservative depends upon the evaporation regime (water- or energy-limited) and the fractional vegetation cover. Their study also showed that the soil component of the EF can be safely assumed to be constant, in contrast to the canopy component. In their subsequent study (Gentine, Entekhabi, & Polcher, 2011), it was found that the daytime conservation of the EF curve occurs primarily under conditions of high relative humidity and solar radiation on clear-sky days. At lower levels of incoming solar radiation, the EF assumes parabolic and convex patterns during the day. Despite the doubts raised regarding its validity, the EF conservation method has been widely applied in the temporal upscaling of remotely sensed instantaneous ET (Gómez et al., 2005; Sobrino, Gómez, Jiménez-Muñoz, & Olioso, 2007; Galleguillos, Jacob, Prévot, Lagacherie, & Liang, 2011).

Another ET upscaling method was introduced by Trezza (2002) to incorporate the effect of horizontal advection and variable environmental factors on the EF in a diurnal cycle. This method is the so-called constant reference evaporative fraction (EF_r, the ratio of actual to reference grass/alfalfa ET) method. The EF_r method assumes that the ratio of the actual instantaneous LE to the daily LE can be represented by the ratio of the corresponding reference instantaneous LE to the daily LE, where the reference LE is the evapotranspiration from a reference surface (e.g., grass/alfalfa) that is not short of water and has specific characteristics (Allen, Pereira, Raes, Raes, & Smith, 1998; Allen et al., 2006). The conception of EF_r is similar to the definition of the crop coefficient (K_c) that is widely used in agricultural water resources management (Allen et al., 1998). By analogy with the EF conservation method, the daily ET is obtained by multiplying the EF_r by the daily reference ET. Previous studies have stated that maintaining the conservation of EF_r in a diurnal cycle could provide better estimates of the daily ET under the advective conditions that usually occur in the afternoon (Trezza, 2002; Allen, Tasumi, & Trezza, 2007).

Other representative alternatives to the constant EF and EF_r methods for upscaling the instantaneous ET include those that attempt to relate the ratio of instantaneous to daily ET to variations of the diurnal global solar radiation, the extraterrestrial solar radiation, and the surface net radiation because these sources of radiation are the primary energy drivers of surface water and energy transfer on the land surface. For example, Jackson, Hatfield, Reginato, Idso, and Pinter (1983) proposed a sinusoidal variation of global solar radiation to extrapolate the instantaneous LE. Brutsaert and Sugita (1992) examined the constant flux ratios of surface available energy (EF conservation) and global solar radiation, respectively, in deriving the daytime total LE and showed that both ratios could provide good results in reproducing the daytime ET estimates but with an underestimation of 5–10%. Ryu et al. (2012) recently adopted the ratio of instantaneous to daily extraterrestrial solar radiation to upscale the remotely sensed ET to daily and eight-day averaged values. By testing their results against eddy covariance measurements from 34 instrumented towers in North America and Europe, they found that this ratio was a robust scaling factor in comparison with the EF conservation method.

It appears that all the upscaling methods cited above can be effectively used to convert the instantaneous (or half-hourly and hourly) ET to a daytime/daily value, as reported in different studies by the numerous authors. Unlike the constant reference evaporative fraction method, the EF conservation method and the constant flux ratio (e.g., the extraterrestrial solar radiation ratio) methods cannot capture the effects of horizontal advection and atmospheric environmental factors (e.g., wind speed, vapor pressure deficit) on the variations of the diurnal flux (available energy or the extraterrestrial solar radiation) in the daily LE estimation. However, in the reference evaporative fraction method, the reference ET estimated from the Penman–Monteith equation (Monteith, 1965) requires as input the air temperature, the relative humidity, the solar radiation, and the wind speed, which may introduce a degree of uncertainty into the estimated daily total LE. Moreover, the possible lack of these detailed meteorological hourly data may hinder the broad application of the reference evaporative fraction method.

The performance of these aforementioned ET upscaling methods has been evaluated by some authors in previous studies (Brutsaert & Sugita, 1992; Colaizzi, Evett, Howell, & Tolk, 2006; Chávez, Neale, Prueger, & Kustas, 2008; Delogu et al., 2012; Ryu et al., 2012). Consistent conclusions have rarely been drawn, primarily because these comparisons differ in the use of modeled or observed fluxes as the upscaling factor, in the upscaling of instantaneous ET to daytime or daily integrated values, and in the application of the upscaling methods under very limited clear sky or all sky conditions. Van Niel et al. (2012) used modeled global solar radiation, modeled extraterrestrial solar radiation, observed global solar radiation, and observed surface available energy as the upscaling factors to test their ability in converting the instantaneous ET to daily values on selected days over a ~10-year period. Their findings suggest that using observed global solar radiation as the upscaling factor performs best in deriving daily ET. However, the constant reference evaporative fraction method that can account for the variations of the meteorological variables in a diurnal cycle is not involved in their upscaling methods and therefore needs to be further tested together with these upscaling factors.

The objective of this study is to comprehensively evaluate the performance of four commonly used ET-upscaling methods in converting remotely sensed instantaneous ET to daily (24-h) averaged values. This objective involves the use of long-term ground-based measurements obtained from an eddy covariance (EC) system on clear-sky days and partly cloudy days. These measurements were collected at the Yucheng comprehensive experimental station in Northern China spanning the period from late April 2009 to late October 2011. An intercomparison of the four upscaling methods at different time intervals from mid-morning (9:00 local time) to mid-afternoon (15:00 local time) is made using ground-based measurements and satellite estimates to clearly recognize the intrinsic and extrinsic uncertainties and errors in the extrapolation to daily and longer time-scale estimates of ET. The contribution of this paper primarily lies in analyzing the different upscaling methods on both closed and un-closed surface fluxes and over different assumed satellite overpass times from mid-morning to mid-afternoon. Moreover, the data included in

the analysis cover a broad range of both soil wetness/vegetation cover and environmental forcing from late April 2009 to late October 2011. This study is conducted to provide a scientific basis for the development of an operational and more accurate ET-upscaling method with easy data access in our future work. In Section 2, a brief description of the formulations of the four ET upscaling methods is provided, and a well-known two-source model of instantaneous ET estimation from remote sensing data is outlined. An experimental design is also described in this section. In Section 3, the validation site, the ground-based EC measurements for analysis, the relevant Moderate Resolution Imaging Spectroradiometer (MODIS) remote sensing data for instantaneous ET estimation, the procedures to select the clear sky days and partly cloudy days, and the energy imbalance correction method are presented. In Section 4, the four ET upscaling methods for converting instantaneous EC-measured LE and satellite estimates to daily values are intercompared. A summary and conclusion are provided in Section 5.

2. Model descriptions

2.1. ET upscaling method

As stated above, the scheme used to upscale the instantaneous remote sensing estimates of ET generally requires that the daily (24-h) averaged LE (or ET) be related to a factor that can be nearly constant over a diurnal cycle,

$$\frac{LE_i}{LE_d} = \frac{ET_i}{ET_d} = \frac{\Omega_i}{\Omega_d} \tag{1}$$

where Ω can be (for example) the surface available energy, the extraterrestrial solar radiation, the global solar radiation, or the reference ET. The subscripts "i" and "d" represent the instantaneous and daily averaged values, respectively.

2.1.1. Constant evaporative fraction method

If Ω in Eq. (1) equals the surface available energy, the upscaling scheme is called the constant evaporative fraction method (Shuttleworth et al., 1989; Brutsaert & Sugita, 1992).

2.1.2. Constant extraterrestrial solar radiation ratio method

If Ω in Eq. (1) equals the extraterrestrial solar radiation (R_a), the upscaling scheme is called the constant extraterrestrial solar radiation ratio ($R_p = LE_i/R_{a,i}$) method (Ryu et al., 2012).

The extraterrestrial solar radiation at daily and hourly or shorter periods on a given day can be estimated from the solar constant, the geographic latitude, the solar declination, the day of year, and the time of day (Allen et al., 1998),

$$R_{a,d} = \frac{1440}{\pi} G_{sc} d_r (\omega_s \sin(\varphi)\sin(\delta) + \cos(\varphi)\cos(\delta)\sin(\omega_s)) \tag{2}$$

$$R_{a,i} = \frac{720}{\pi} G_{sc} d_r ((\omega_2 - \omega_1)\sin(\varphi)\sin(\delta) + \cos(\varphi)\cos(\delta)(\sin(\omega_2) - \sin(\omega_1))) \tag{3}$$

where G_{sc} is the solar constant, 0.082 MJ/(m^2 · min); d_r is the inverse relative Earth–Sun distance; ω_s is the sunset hour angle, rad; φ is the latitude, rad; δ is the solar declination, rad; ω_1 is the solar time angle at the beginning of the hourly (or shorter) period, rad; and ω_2 is the solar time angle at the end of the hourly (or shorter) period, rad.

2.1.3. Constant global solar radiation ratio method

If Ω in Eq. (1) equals the global solar radiation (R_s), the upscaling scheme is called the constant global solar radiation ratio ($R_g = LE_i/R_{s,i}$) method.

2.1.4. Constant reference evaporative fraction method

If Ω in Eq. (1) equals the reference crop ET (ET_r), the upscaling scheme is called the constant reference evaporative fraction ($EF_r = LE_i/ET_{r,i}$) method (Trezza, 2002; Allen et al., 2007).

The reference ET is estimated from the Penman–Monteith equation for a hypothetical grass with an assumed height of 0.12 m having a surface resistance of 50 s/m during daytime and 200 s/m during nighttime and an albedo of 0.23, as suggested by ASCE-EWRI (2005),

$$ET_r = \frac{0.408\Delta(R_n - G) + \gamma \frac{C_n}{T_a + 273} u_2 (e_s - e_a)}{\Delta + \gamma(1 + C_d u_2)} \tag{4}$$

where Δ is the slope of the saturated vapor pressure vs. air temperature curve, kPa/°C; R_n is the surface net radiation, W/m^2; G is the soil heat flux, W/m^2; γ is the psychrometric constant, kPa/°C; C_n equals 900 at a daily time scale and 37 at an hourly scale; e_s–e_a is the vapor pressure deficit of the air, kPa; T_a is the air temperature, °C; C_d equals 0.24 during daytime and 0.96 during nighttime; and u_2 is the wind speed at a 2 m height, m/s. The calculation of each of the variables in Eq. (4) here closely follows the procedure specified by ASCE-EWRI (2005). The daily (24-h) ET_r is estimated by averaging the half-hourly value as derived by Eq. (4) in a diurnal cycle.

The performance of Eq. (1) in upscaling ET depends on how closely the instantaneous flux ratio at a given clear sky time represents that at the daily scale. Intermittent clouds during daytime decrease the observed global solar radiation and, thus, the surface available energy that is used for energy partitioning into latent heat flux. The effect of clouds on the observed global solar radiation has been clearly incorporated in the constant EF, R_g, and EF_r methods but is not identified in the constant R_p method. The amount and duration of cloud cover during daytime will pose a challenge to the validity of Eq. (1) and consequently affect the accuracy of the upscaling methods.

2.2. Two-source energy balance model

The remote sensing model used in this study for instantaneous ET estimation is the two-source energy balance (N95) model originally developed by Norman, Kustas, and Humes (1995). This model can partition the energy fluxes and surface temperature into soil and vegetation components and is relatively less sensitive to atmospheric and vegetation inputs (e.g., air temperature, wind speed, relative humidity, global solar radiation, leaf area index, vegetation height, and surface temperature) than the commonly used one-source bulk transfer models. This two-source model has been shown to be robust in the estimation of soil and canopy evapotranspiration for a wide range of landscape and hydrometeorological conditions (Kustas & Norman, 1997; Choi et al., 2009; Tang et al., 2011; Cammalleri et al., 2012). The remarkable superiority of the N95 model is that it can incorporate the satellite view geometry and avoid the empirical correction of the excess resistance without requiring more inputs than conventional one-source energy balance models. Kustas and Norman (2000) subsequently modified the N95 model to estimate the surface net radiation through a more physically based algorithm.

The soil and vegetation temperature and energy components in the N95 model are estimated by making solutions to a series of equations that govern the energy and heat transfer between land surface and atmosphere for both soil and vegetation. The inputs to the N95 model primarily consist of remote sensing data (directional surface temperature, view zenith angle, fractional vegetation cover or leaf area index), ground-based vegetation data (vegetation height, clumping factor), and near-surface atmospheric variables (global solar radiation, air temperature, actual vapor pressure, and wind speed). The remote sensing data used in this study came from the MODIS products. Because the MODIS temperature was likely underestimated/overestimated due to inaccurate atmospheric correction and pixel shift/geolocation error, it

was compared with the temperature estimated from the simultaneous ground-based longwave radiation measurement and correction was made to provide the most accurate inputs for driving the N95 model. The vegetation height and atmospheric variables were from the ground-based measurements at the Yucheng station. The clumping factor, which can be estimated as a function of view zenith angle and the ratio of vegetation height versus width of clumps, was assumed to be 1 due to the lack of necessary information. Details on the parameterization of the variables and the solution of the N95 model can be found in Norman et al. (1995) and Tang et al. (2011).

2.3. Experimental design

In this study, we first assessed the performances of the four upscaling methods as shown in Section 2.1 in upscaling instantaneous LE to daily (24-h) ET solely based on ground-based half-hourly measurements with and without the energy imbalance correction, which can separate the errors induced by the methods from those by the inputs. This assessment was made at different hourly time intervals (the assumed different satellite overpass times) from mid-morning (9:00 local time) to mid-afternoon (15:00 local time) for the clear sky and partly cloudy days.

After the assessment solely based on the ground-based measurements, the four upscaling methods were assessed by upscaling the instantaneous LE derived from the two-source N95 model, which can quantify the accuracy of the upscaled daily LE by introducing the error incurred by the instantaneous LE estimation. In this assessment, the instantaneous LE was estimated by applying the N95 model to MODIS data at the Yucheng station.

During the above assessments, daily global solar radiation and daily surface available energy as required by the constant R_g method and the constant EF method, respectively, were derived by averaging the half-hourly measurements over a 24-h period while daily extraterrestrial solar radiation required by the constant R_p method was modeled. For the constant EF_r method, the daily ET_r was obtained by averaging the half-hourly estimates of ET_r over a 24-h period with all the inputs coming from the ground-based measurements.

We used the 24-h integrated global solar radiation and surface available energy measurements in the upscaling of remote sensing instantaneous LE rather than estimating them from models mainly because 1) most of their estimation methods have difficulty in estimating the daily shortwave atmospheric transmissivity, especially on partly cloudy days and 2) the methods to estimate daily global solar radiation, daily surface available energy, daily extraterrestrial solar radiation, and daily ET_r are different in both input and accuracy. Overestimation or underestimation of these daily averaged variables will inevitably deteriorate the comparisons of the daily ET even if the upscaling methods are accurate. Therefore, it may be better to minimize the effect of these daily averaged variables on the upscaled daily ET to more clearly quantify how well each of the upscaling methods performs in upscaling the remote sensing instantaneous LE.

3. Test site and satellite data

3.1. Test site

The test site at which ground-based atmospheric variables are collected for the analysis is located at the Yucheng comprehensive experimental station (hereafter, called the Yucheng station), at latitude and longitude 36.8291° N and 116.5703° E, respectively, in Northern China. The Yucheng station was established as part of the Chinese terrestrial ecosystem flux research network (ChinaFlux) to measure the long-term exchange of water, energy, and carbon dioxide between the land ecosystem and the atmosphere (http://www.chinaflux.org/). The soil is sandy loam, and the land cover near the Yucheng station primarily consists of crop (winter wheat and summer corn rotation), bare soil, trees, and water, as shown in the classification map from the TM data in Fig. 1a. The site has a subhumid monsoon climate with a mean annual temperature and precipitation of 13.1 °C and 582 mm, respectively. Approximately 60–70% of the rainfall occurs in the summer corn growing season and the remaining 30–40% occurs in the winter wheat season.

An eddy covariance (EC) system consisting of an open-path CO_2/H_2O gas analyzer (model LI-7500, Licor Inc., Lincoln, Nebraska, USA) and a 3-D sonic anemometer/thermometer (model CSAT3, Campbell Scientific Inc., Logan, Utah, USA) was installed at the Yucheng station to regularly measure 30-min averaged turbulent sensible heat flux (H) and latent heat flux. The measurement height above the ground surface was increased to ~4.3 m in late July or early August and decreased to ~2.9 m in mid- to late October each year. A series of common corrections for the effect of the sonic virtual temperature, the time-lag, the performance of the planar fit coordinate rotation, the density fluctuation, and the frequency response was made to obtain reliable EC-measured sensible heat flux and latent heat flux using the online flux

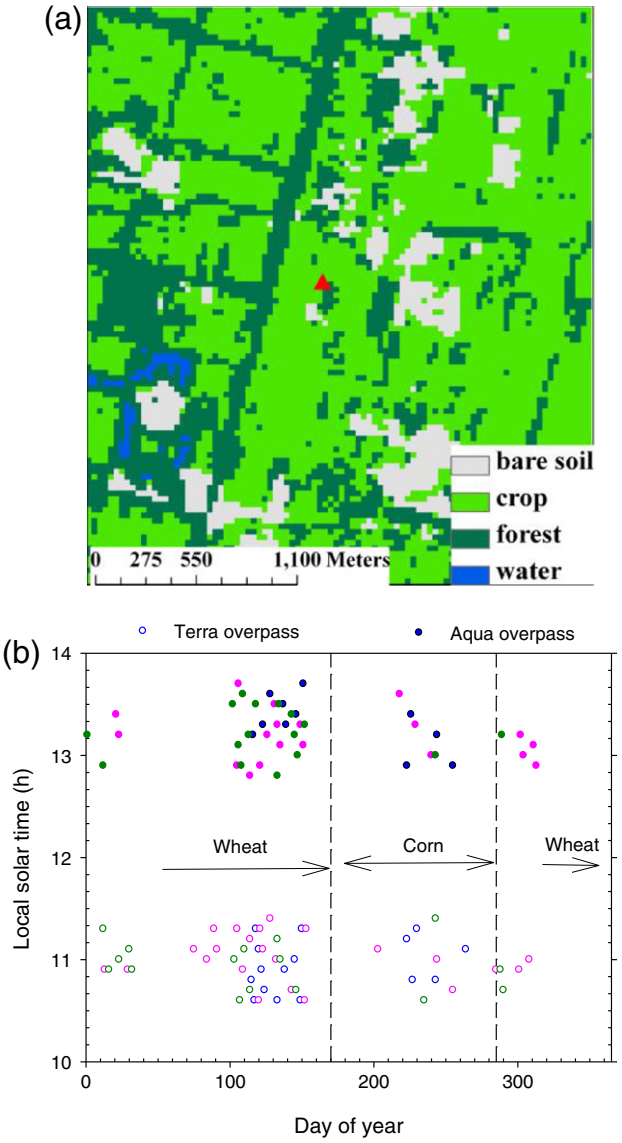

Fig. 1. (a) Land cover classification from TM data acquired on 30th August, 2009 near the Yucheng station as indicated by the filled red triangle in the center, (b) temporal distribution of the 55 MODIS/Terra and 46 MODIS/Aqua clear sky overpass times from April 2009 to October 2011 selected for the instantaneous ET estimation from the remote sensing model (blue: 2009, pink: 2010, dark green: 2011).

computation and post-field data programs (Webb et al., 1980; Burba & Anderson, 2010). Downwelling and upwelling shortwave and longwave radiations were measured using a CNR-1 device (Kipp & Zonen, Delft, Netherlands), and the soil heat flux was measured using a single HFP-01 soil heat flux plate (HukseFlux, Delft, Netherlands) at a soil depth of 2 cm. Heat storage above the plate was not considered. All the meteorological variables and EC measurements were made in an experimental area with dimensions of approximately 250 m by 90 m at the Yucheng station. The experimental area has the same crop type as the surrounding farmland and is relatively uniform (Fig. 1a).

Half-hourly averaged atmospheric variables (global solar radiation, surface net radiation, soil heat flux, air temperature, wind speed, relative humidity, and atmospheric pressure) and ground-based crop height (interpolated from the periodical measurements that were collected every ~10 to ~20 days) from late April 2009 to late October 2011 were collected to drive the N95 model and the daily (24-h) averaged latent heat flux measured by EC with and without energy imbalance correction to validate the value extrapolated from the four upscaling methods. These data were carefully checked to ensure quality and completeness by 1) removing data spikes and abnormalities (H and LE less than -100 W/m^2 or greater than 700 W/m^2, approximating the lower and upper limits of surface net radiation) in the measured sensible heat flux and latent heat flux and then 2) excluding days when data gaps, e.g., caused by rainfall events or instrument malfunction or maintenance, were observed in the 30-min averaged atmospheric variables or EC-measured sensible and latent heat fluxes. After these quality control steps, the daily measured surface fluxes (surface net radiation, soil heat flux, sensible heat flux, and latent heat flux) for the evaluation of the four upscaling methods were derived by averaging the 48 half-hourly measurements in a diurnal cycle.

3.2. MODIS data

The satellite data used in this study for instantaneous ET estimation from the N95 model were obtained from the MODIS/Terra and MODIS/Aqua platforms. The Terra and Aqua satellites view the entire surface of the Earth every one to two days. The onboard MODIS instrument has 36 discrete spectral bands between 0.405 μm and 14.385 μm and acquires data at three spatial resolutions: 250 m, 500 m, and 1000 m. The MODIS products can be freely downloaded from the Land Processes Distributed Active Archive Center (LP DAAC, https://lpdaac.usgs.gov/get_data).

The MODIS data used in this study are the Land Surface Temperature (LST) and Emissivity 5-min L2 Swath 1 km data set product (MOD11_L2 for the Terra satellite and MYD11_L2 for the Aqua satellite) produced using the generalized split-window LST algorithm (Wan & Dozier, 1996; Li et al., 2013a), the geolocation dataset product (MOD03 and MYD03) at a 1 km spatial resolution, and the Leaf Area Index (LAI) and Fractional Photosynthetically Active Radiation (FPAR) product (MOD15 and MYD15). The daytime surface temperature and view time in the MOD11_L2 and MYD11_L2 products, the solar zenith and satellite view zenith angles in the MOD03 and MYD03 products, and the LAI in the MOD15 and MYD15 products were extracted as part of the input for the remotely sensed N95 model for instantaneous ET estimation.

Because the satellite view geometry has a significant effect on the accuracy of the retrieved land surface temperature (Hall, Huemmrich, Goetz, Sellers, & Nickerson, 1992; Li, Stoll, Zhang, Jia, & Su, 2001; Li et al., 2004; Li et al., 2013a; Tang et al., 2013), the MODIS data in this study were restricted to those having a view zenith angle less than 45° to minimize the angular effect. Moreover, because LAI measurements from MOD15 and MYD15 products estimate only the green leaf area of the vegetation, the application of the N95 model was carried out during the wheat and corn growing periods, excluding the harvest stage when senescent and dead leaves dominate. Constrained by the cloud conditions at the satellite overpass time, the view zenith angle, and the gaps in the ground-based measurements at the Yucheng station, the MODIS data at 55 Terra overpass times and 46 Aqua overpass times (see Fig. 1b) were finally acquired for use in the N95 model for the period from late April 2009 to late October 2011. The maximum and average gaps in the two available successive images were 114 days and ~17 days at the Terra overpass times, respectively, and were 131 days and ~20 days at the Aqua overpass times, respectively.

3.3. Selection of the clear sky and partly cloudy days

Clear sky and partly cloudy days were screened out from the quality and completeness controlled days ($N = 404$) to test the differences in the performance of the upscaling methods. To find an optimal correspondence for the satellite overpass, the performance of the upscaling methods at different time intervals from mid-morning to mid-afternoon was intercompared. Note that the only constraint to the application of the various ET upscaling methods is that they are usually applied on days that are clear during the satellite overpass time. It was therefore necessary to further screen out the partly cloudy days that had clear skies at the different time intervals. The procedures for screening out the clear sky and partly cloudy days were conducted within the above contextualized framework and were presented below:

(i) If both the observed half-hourly global solar radiation and the corresponding shortwave atmospheric transmissivity (τ, the ratio of the observed global solar radiation to the extraterrestrial solar radiation) on a given day increased monotonically from sunrise (global solar radiation >5 W/m^2) to midday and decreased monotonically from midday to sunset (global solar radiation >5 W/m^2), this day was classified as a clear sky day. The selected clear sky days were further visually checked to exclude those that had constant cloud cover during daytime. After these two steps, 31 totally clear sky days (all characterized by a smooth quasi-sinusoidal shape of the observed global solar radiation during daytime) were finally selected to analyze the upscaling methods at each of the time intervals.

(ii) If the observed half-hourly global solar radiation on a given day did not increase monotonically from sunrise to midday or decrease monotonically from midday to sunset, this given day was classified as a partly cloudy day. Because τ varies with solar zenith angle and total column water content, the slant-path τ at a given time interval (e.g., 9:00–10:00 am) on a given partly cloudy day and on two adjacent clear sky days was first converted to a value at the vertical path ($\tau_0 = \tau^{\cos\theta}$, θ is the solar zenith angle) for the selection of the partly cloudy days that were clear sky at the given time interval. If τ_0 at the given time interval for the partly cloudy day was larger than the minimum of the τ_0 at the same time interval on the two adjacent clear sky days, the partly cloudy day would be chosen for further analysis; otherwise, it would be abandoned. Finally, the number of partly cloudy days having clear skies at the 9:00–10:00, 10:00–11:00, 11:00–12:00, 12:00–13:00, 13:00–14:00, and 14:00–15:00 intervals was 48, 45, 28, 38, 41, and 39, respectively.

It is important to note that some clear sky days and/or partly cloudy days may be missing from the automatic procedures presented above. If we were uncertain about whether a given day was clear sky or partly cloudy (e.g., a day characterized by a non-smooth quasi-sinusoidal shape of the observed global solar radiation during daytime) through the procedures, that day would be abandoned to make the comparison of the upscaling methods under clear sky and partly cloudy conditions more reliable and convincing.

3.4. Energy imbalance correction of EC measurements

A number of studies have reported the phenomenon of the energy imbalance in the EC-measured surface energy components ($H + LE < R_n - G$) (Twine et al., 2000; Wilson et al., 2002; Foken, 2008; Stoy et al., 2013). Because most remote sensing models estimate the instantaneous ET based on the surface energy budget, it is necessary to evaluate the four ET upscaling methods under the assumption of the energy closure of ground measurements. Twine et al. (2000) proposed two schemes that have been widely applied to correct the imbalance of the daytime surface energy measurements. One scheme is the Bowen ratio (BR) correction method and the other is the residual energy (RE) correction method. In the BR correction method, the surface available energy is repartitioned into H and LE by conserving the original Bowen ratio measured by EC. In the RE correction method, the imbalanced energy is completely included in the LE. The BR and RE correction methods have been widely applied in a number of papers for validating turbulent heat fluxes of LE and H estimated from diverse models of remote sensing ET (Anderson et al., 2008; Li, Kustas, Anderson, Prueger, & Scott, 2008; Sánchez et al., 2008). Note that the two energy correction methods may be inappropriate if the imbalance is caused by horizontal advection. Moreover, the scale mismatch of the source areas of the energy components (Wu & Li, 2009), the measurement error in the energy components, the length of the sampling intervals, the sensor separation, the dispersive flux not sampled by the EC system, and neglect of the heat storage energy for photosynthesis can all cause an energy imbalance.

Because there was no consensus on how best to reconcile the non-closure in the EC measurements, despite the dispute over the BR and RE correction methods, they were each used to correct the 30-min averaged EC measurement in this study to further evaluate the four upscaling methods. For the application of both the BR and the RE correction methods to the daytime measurements, we assumed the ratio of the daytime to daily LE measured by EC before and after correction to be invariant in deriving the corrected daily LE measurement. Specifically, each of the 30-min averaged LEs measured by EC before correction during daytime is first corrected with the BR or RE correction method. With the assumption that the ratio of the daytime to daily LE measured by EC before and after correction remains invariant, the corrected daily LE can then be derived by dividing the daytime LE measured by EC after correction by the ratio of the daytime to the daily LE measured by EC before correction. This assumption also implies that the ratio of the nighttime to daytime ET remained unchanged before and after correction. The motivation for this assumption was that when we directly applied the BR and RE correction methods to each of the corresponding 30-min averaged LE measurements in a diurnal cycle, the daily LE after correction averaged over the clear sky and partly cloudy days was shown to be less than that before correction for the RE correction method due to the negative available energy in the nighttime. Moreover, the BR correction method was corrupted if the sum of the original H and LE was close to zero in the nighttime.

4. Results and discussion

4.1. Daytime variation in the upscaling factors

Before we evaluated the performance of the four upscaling schemes in extrapolating the instantaneous ET to the daily value, the daytime variation of the half-hourly surface energy components, the estimated ET_r, and the upscaling factors, averaged over 31 selected clear sky days and 28 selected partly cloudy days when there was clear sky from 11:00 to 12:00 local time, was examined, as shown in Fig. 2a–d. The smooth sinusoidal shape of the surface net radiation (R_n) was clearly shown for the clear sky days. The decrease of the R_n caused by the effect of the clouds at the different time intervals was largely averaged out for the partly cloudy days. For both clear sky and partly cloudy days, the EC-measured LE was shown to be the largest energy component in the partitioning of R_n because of the high rainfall and soil water content at the Yucheng station, and it was greater than the estimated ET_r due to the different functioning of stomatal control on the real crops and on the reference grass. Both the EC-measured LE and the estimated ET_r closely followed the variation of the main driving energy. All four upscaling factors (EF_r, EF, R_p, and R_g) near midday showed less variation under the clear-sky conditions than under the partly cloudy conditions. The standard deviations of the EF_r, EF, R_p, and R_g during the period 10:00 h–14:00 h were 0.030, 0.020, 0.008, and 0.009, respectively, for the clear-sky days and 0.043, 0.028, 0.011, and 0.013, respectively, for the partly cloudy days. The conservation of the EF near the midday as reported in previous studies was verified. The EF_r, R_p, and R_g ratios were also relatively conservative during this period on the clear sky days. It was evident that cloud cover increased the standard deviation of all four upscaling ratios on the partly cloudy days and made them less conservative.

The EF factor systematically underestimated the daily average from mid-morning (9:00 local time) to mid-afternoon (15:00 local time). In particular, the EF at the 11:00–12:00 interval when there was clear sky on the partly cloudy days was obviously smaller than that at the other time intervals, indicating that EF would increase if clouds were present; this would result in a greater underestimation of the daily ET under partly cloudy days than under clear sky days for the EF method. On the clear sky days, the EF_r factor was shown to be larger in the mid-morning and smaller in the mid-afternoon than the daily average, whereas underestimation in the mid-morning and overestimation in the mid-afternoon were found for the R_p and R_g factors when compared to their daily averages. The difference between the EF, R_p, and R_g factors at the clear sky time (11:00–12:00) and their daily averages on the partly cloudy days was shown to increase due to the presence of clouds, indicating that more deviations would appear in the daily ET estimates from these three upscaling factors on the partly cloudy days than under the clear sky days. The clouds evidently impacted the performance of the R_p factor in the daily ET estimates. The performance of the EF_r factor can also be influenced by clouds, but not as significantly, mainly because the effect of clouds on the observed global solar radiation can be incorporated into the half-hourly and daily ET_r estimates. Under both clear-sky and partly cloudy conditions, the four half-hourly upscaling factors from noon to mid-afternoon showed relatively better agreement with the daily averages estimated as the ratio of the sum of the half-hourly EC-measured LE to the sum of the half-hourly ET_r (or R_n–G or R_a or global solar radiation) in a diurnal cycle. The mean absolute value of the relative BIAS of the four upscaling factors relevant to the daily averages during the mid-morning to the mid-afternoon followed the order $EF > R_p > R_g > EF_r$ (33%, 5%, 3%, and 1%, respectively) on the clear sky days. The absolute relative BIAS relevant to the daily averages for clear sky at 11:00–12:00 is $EF > R_g > EF_r > R_p$ (33%, 13%, 4%, and 0%, respectively) on partly cloudy days. Note that the R_p happened to approximate the daily averages at the 11:00–12:00 interval on the partly cloudy days, but there were great differences at other time intervals.

4.2. Evaluation using original flux tower measurements

To minimize the effect of the uncertainty in the instantaneous ET estimated from remotely sensed models, the four upscaling schemes described in Section 2.1 were evaluated first using completely the ground-based measurements of the atmospheric variables, surface net radiation, soil heat flux, and EC-measured sensible heat flux (H) and latent heat flux (LE) at the Yucheng station on the clear sky days and partly cloudy days selected in Section 3.3. In addition, the EC-measured daily LE was compared with the upscaled values at different time intervals from mid-morning (9:00 local time) to mid-afternoon (15:00 local time) to find the best correspondence with the overpass time of the satellite.

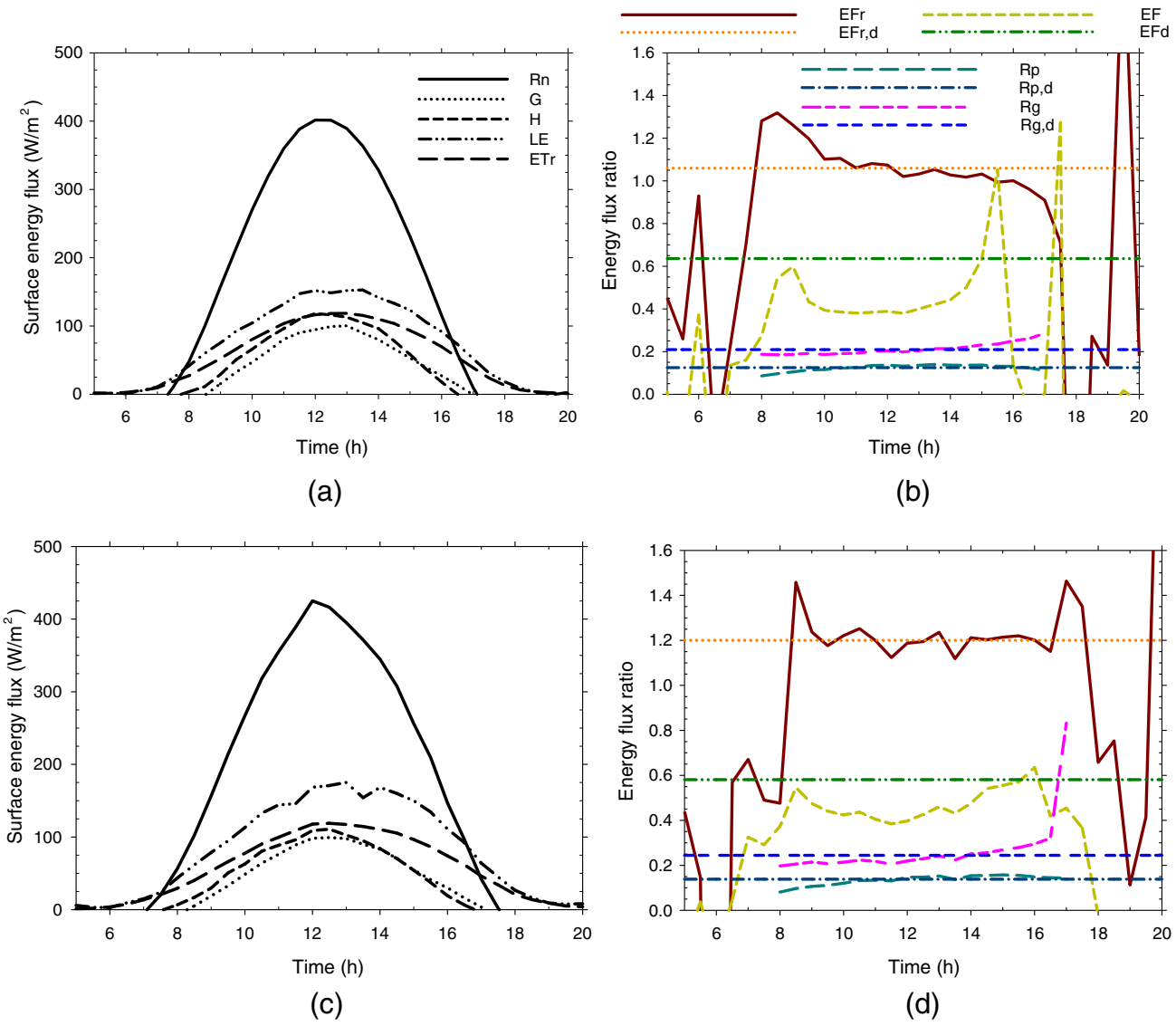

Fig. 2. Daytime variation of ground-based measurements of surface net radiation (R_n), soil heat flux (G), sensible heat flux (H), latent heat flux (LE), reference ET (ET_r), reference evaporative fraction (EF_r), evaporative fraction (EF), extraterrestrial solar radiation flux ratio (R_p), and observed global solar radiation flux ratio (R_g), and daily (24-hour) mean at the Yucheng station. (a–b) Averaged over all of the selected clear-sky days (N = 31), (c–d) averaged over selected partly cloudy days (N = 28) when it is clear sky during 11:00 to 12:00 am.

Fig. 3a–f shows the results of the comparison with the instantaneous ET derived as the hourly averages for the six time intervals (9:00–10:00, 10:00–11:00, 11:00–12:00, 12:00–13:00, 13:00–14:00, and 14:00–15:00) on the 31 clear-sky days for the EF_r, EF, R_p, and R_g methods. The corresponding statistical measures of the performance of the four upscaling schemes are presented in Fig. 4a–c. The positive and negative BIAS (the difference between the estimated and observed daily LE) indicate that the estimated daily LE was higher and lower than the observed value, respectively. Several findings are summarized as follows. (i) Using EF_r to upscale LE tended to give the lowest absolute BIAS and root mean square error (RMSE) for all the time intervals from mid-morning to mid-afternoon. This means when detailed ground-based meteorological data are available, the EF_r factor will be the best to upscale LE under clear sky days. Note that even if the multi-day averaged EF_r was larger (smaller) than the multi-day daily average, it does not mean that the averaged daily LE would be overestimated (underestimated) because the upscaled daily LE was controlled by both the EF_r and the ET_r estimates. (ii) Using EF as the upscaling factor gave the highest absolute BIAS and RMSE and underestimated the daily LE (negative BIAS) for all time intervals, but the underestimation decreased from mid-morning to mid-afternoon. This means the mid-afternoon period may be the best time to upscale LE when using EF as the upscaling factor under clear sky days. (iii) Using R_p to upscale LE gave a lower absolute BIAS and RMSE in the mid-morning and a higher BIAS and RMSE in the mid-afternoon than using R_g. Both the R_p and the R_g upscaling factors had a negative BIAS in the mid-morning and a positive BIAS in the mid-afternoon. The time when the negative BIAS became positive for the R_g factor appeared to lag behind that for the R_p factor. In the mid-morning, the R_p factor performed better than the R_g factor. From noon to mid-afternoon, opposite results were observed. The coefficient of determination (R^2) for all the upscaling methods was higher than 0.94, except for the EF factor, which varied between 0.91 and 0.97. The upscaling of LE near noon compared with that at other times (e.g., mid-morning or mid-afternoon) was able to produce a daily LE that had the best correspondence with the ground-based measurement, at least for the EF_r, R_p, and R_g methods. Therefore, if several satellite overpasses from the morning to the afternoon are available, the overpass at near-noon may be the most suitable for the LE upscaling, at least for the EF_r, R_p, and R_g methods.

To evaluate the impact of clouds during the daytime on the daily LE, Fig. 5a–f compares the four upscaling schemes at the six time intervals

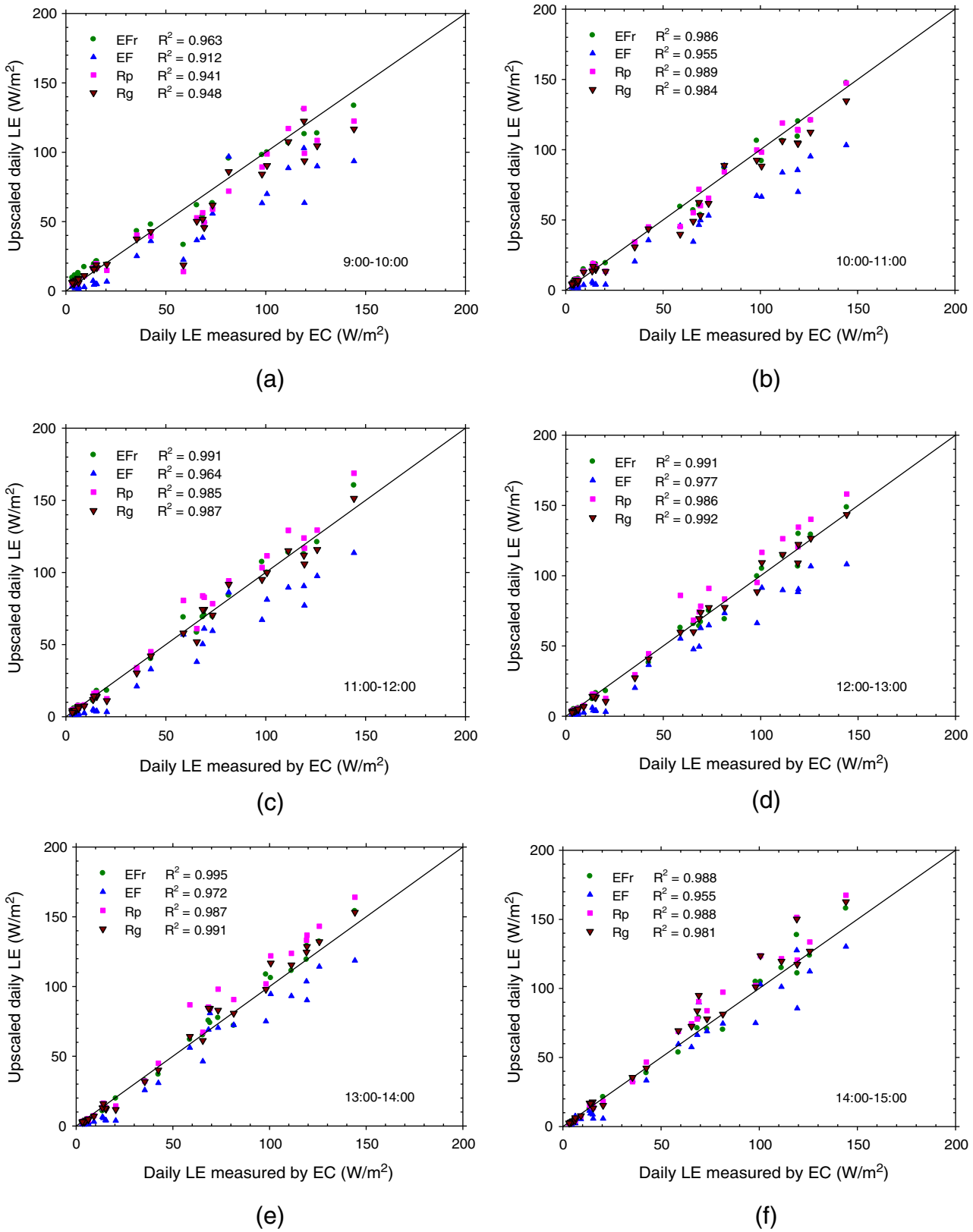

Fig. 3. Comparison of the daily LE measured by eddy covariance system without any energy correction with that derived by the four upscaling methods applied at different time periods in the daytime over 31 clear-sky days. All data were from ground-based measurements collected between late April 2009 and late October 2011 at the Yucheng station. (a) 9:00–10:00, (b) 10:00–11:00, (c) 11:00–12:00, (d) 12:00–13:00, (e) 13:00–14:00, (f) 14:00–15:00.

on the selected partly cloudy days. The corresponding statistical measures are also shown in Fig. 4a–c. Both the absolute BIAS and RMSE for the four upscaling methods had a tendency to increase (with exceptions at the 9:00–10:00 and 11:00–12:00 intervals for the R_p factor) while the R^2 decreased, which means these upscaling methods tend to perform worse under partly cloudy conditions than under clear skies. Same as

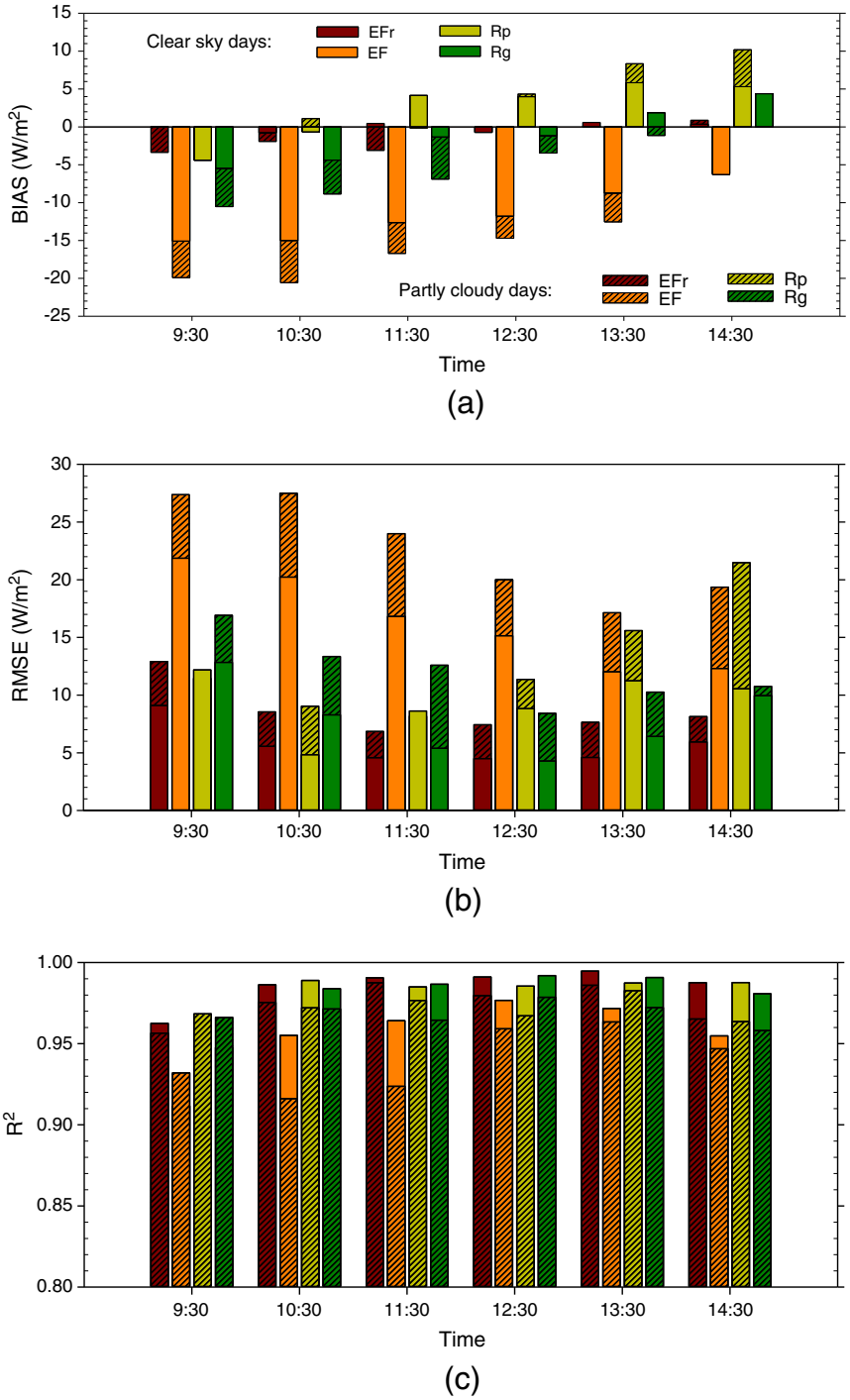

Fig. 4. Statistical measures of the performance of four upscaling methods in converting hourly ET estimated at different clear sky time periods in the daytime to daily value under clear-sky or partly cloudy conditions (9:30 stands for 9:00–10:00 interval, similarly hereafter). The EC-measured LE was not corrected to close the energy imbalance. (a) BIAS, (b) RMSE, (c) R^2.

the results obtained over clear sky days, (i) using EF_r and EF to upscale LE still tended to have the lowest and highest absolute BIAS and RMSE, respectively, for all of the time intervals; (ii) using EF as the upscaling factor still underestimated the daily LE for all time intervals; and (iii) using R_p to upscale LE gave a lower absolute BIAS and RMSE in the mid-morning and a higher BIAS and RMSE in the mid-afternoon than using R_g. On both the clear sky and partly cloudy days, the daily LE upscaled with the R_p factor was shown to be overall larger than that with the R_g factor for all the time intervals. The daily LE had a tendency to be underestimated in the mid-morning and overestimated in the mid-afternoon from these two upscaling factors. Clouds seemed to increase and decrease the daily LE upscaled from the R_p and R_g factors, respectively, making the time when negative BIAS became positive move forward for the R_p factor and backward for the R_g factor.

4.3. Evaluation using corrected flux tower measurements

The underestimation of the original EC-measured daily LE by the EF method was demonstrated in Section 4.2. A possible reason for this outcome was the undermeasurement of half-hourly H and LE by the instrument and the energy imbalance in the measured surface energy components. The closure ratio, defined as the ratio of the sum of H and LE to surface available energy, averaged approximately 0.81 at the half-hourly time scale and 0.89 at the daily time scale over

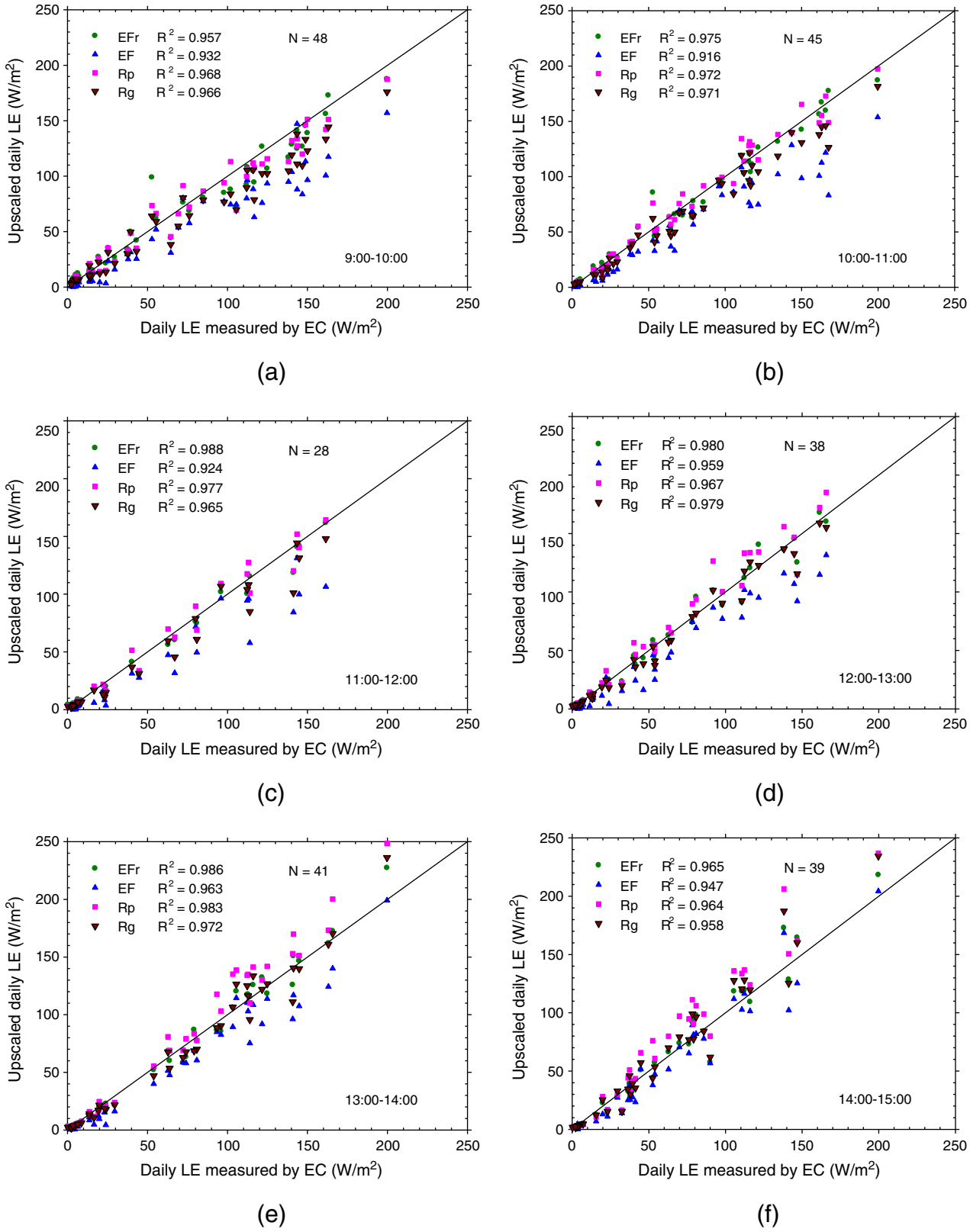

Fig. 5. Comparison of the daily LE measured by eddy covariance system without any energy correction with that derived by the four upscaling methods applied at different clear sky time periods in the daytime over partly cloudy days. All data were from ground-based measurements collected between late April 2009 and late October 2011 at the Yucheng station. (a) 9:00–10:00, (b) 10:00–11:00, (c) 11:00–12:00, (d) 12:00–13:00, (e) 13:00–14:00, (f) 14:00–15:00.

the quality- and completeness-controlled 404 days. It is evident that the closure ratio increased with the longer time integration, and correction to the energy imbalance of the EC measurements seemed more necessary at a shorter time scale.

Fig. 6a–c shows the statistical measures of the performance of the four ET upscaling methods with hourly LE derived at six time intervals using the BR correction method to close the energy imbalance of the original EC measurement for the clear sky and partly cloudy days. On

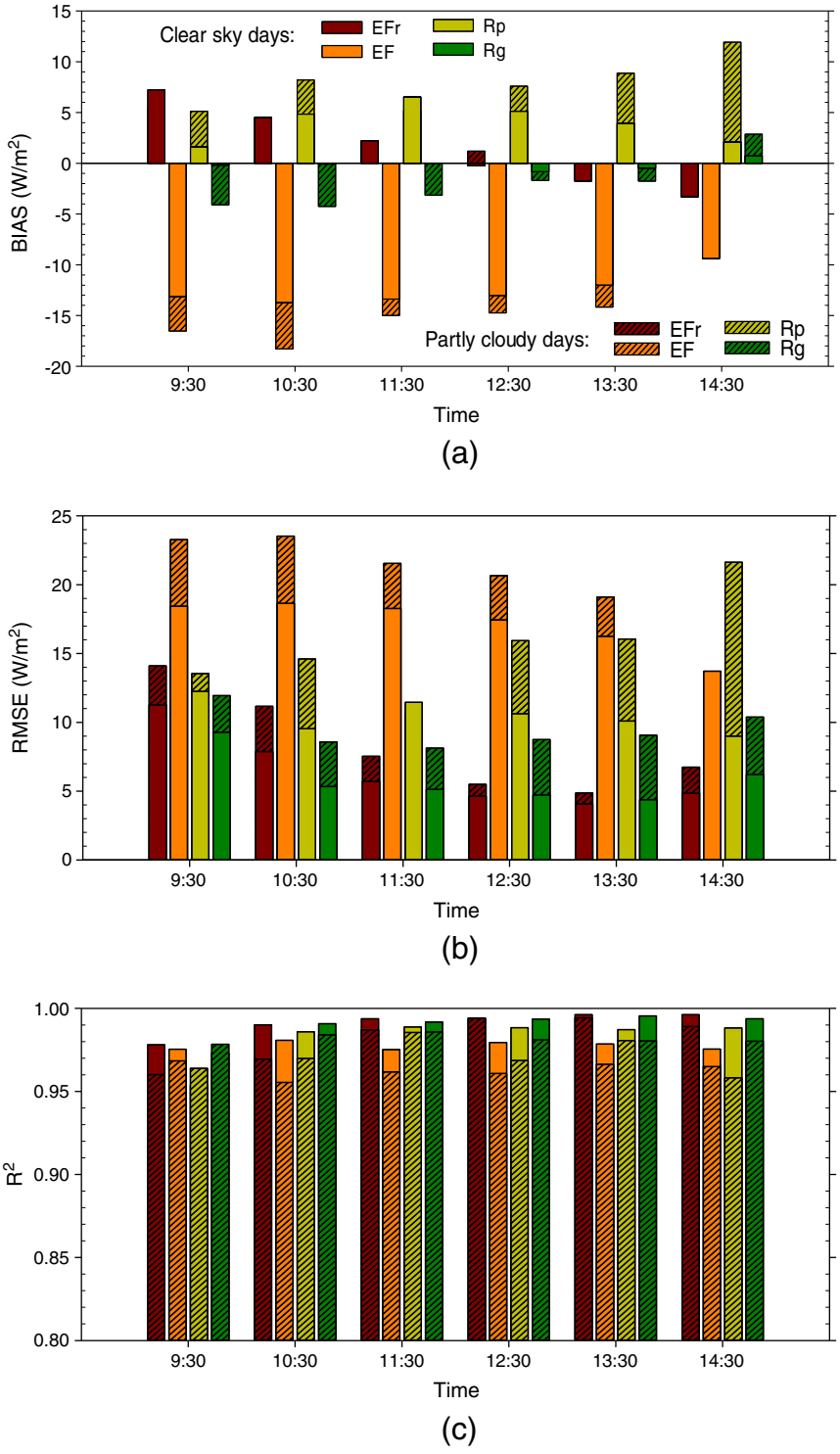

Fig. 6. Same as Fig. 4, but for the application of energy closure of the EC-measured LE using the Bowen ratio correction method.

the clear sky days, the results reveal the following. (i) Using the R_g factor to upscale LE tended to give the lowest absolute BIAS (very close to 0) for all time intervals. (ii) Using the R_g (EF_r) factor to upscale LE tended to give the lowest (second-lowest) RMSE in the mid-morning and the second-lowest (lowest) RMSE in the mid-afternoon. (iii) Using the EF factor to upscale LE gave the largest absolute BIAS and RMSE and underestimated the daily LE for all time intervals. (iv) Using the R_p factor to upscale LE tended to give the second-largest absolute BIAS and RMSE and overestimated daily LE for all time intervals. (v) Using the EF_r factor gave an overestimated daily LE (positive BIAS) in the mid-morning and an underestimated daily LE in the mid-afternoon (negative BIAS). (vi) The RMSE for both the EF_r and the R_g factors to upscale LE first decreased and then increased with time from the mid-morning to mid-afternoon, with the minimum occurring near noon. (vii) No obvious difference was observed in the performance of the R_p upscaling factor at the different time intervals. (viii) All the R^2 are higher than 0.97. (ix) Noon seemed to have the best correspondence with the satellite overpass for the upscaling of LE, at least for the well performed EF_r and R_g methods. On the partly cloudy days, the absolute BIAS and RMSE for all the upscaling factors tended

to increase to a certain degree, except the absolute BIAS for the EF_r factor. This means that the overestimation or underestimation of daily LE for the upscaling factors would become more serious under partly cloudy days if the BR correction method was used to correct the energy imbalance of the EC measurements. Similar to the results obtained on the clear sky days, using the R_g (EF_r) factor to upscale LE tended to yield the lowest (second-lowest) RMSE in the mid-morning and the second-lowest (lowest) RMSE in the mid-afternoon. Using the EF factor to upscale LE gave the largest absolute BIAS and RMSE and underestimated the daily LE for all time intervals (an exception occurred in the mid-afternoon when using the R_p factor performed worst). Using the R_p factor to upscale LE tended to give the second-largest absolute BIAS and RMSE and overestimated the daily LE for all time intervals (an exception occurred in the mid-afternoon, when the absolute BIAS and RMSE were the largest for the R_p factor). The RMSE for both the EF_r and R_g factors to upscale LE first decreased and then increased with time from the mid-morning to mid-afternoon, with the minimum occurring near noon. All the R^2 were higher than 0.95.

Fig. 7a–c shows the statistical measures of the performance of the four ET upscaling methods using the RE correction method to close the energy imbalance of the original EC measurement for the clear sky and partly cloudy days. Overall, using the R_g factor to upscale LE gave the lowest absolute BIAS and RMSE for all time intervals on the clear sky days. However, on the partly cloudy days, using the EF_r factor gave the lowest RMSE from noon to mid-afternoon. On both the clear sky and partly cloudy days, using the EF factor to upscale LE gave the largest absolute BIAS and RMSE (exceptions occurred during the 9:00–10:00 interval on clear sky days and the 14:00–15:00 interval on partly cloudy days) and underestimated the daily LE for all time intervals. Using the R_p factor to upscale LE gave the second-largest absolute BIAS and RMSE and tended to overestimate the daily LE for all time intervals. Using the EF_r factor and the R_g factor first overestimated (positive BIAS) and then underestimated the daily LE from mid-morning to mid-afternoon. The presence of clouds increased the absolute BIAS and RMSE for the EF and R_p factors. The absolute BIAS and RMSE decreased in the mid-morning but increased in the mid-afternoon for the R_g factor when clouds were present. The absolute BIAS was decreased overall for all time intervals and the RMSE was increased in the mid-morning but decreased in the mid-afternoon for the EF_r factor on the partly cloudy days. Almost all the R^2 for the upscaling factors were greater than 0.94 on both the clear sky and partly cloudy days. An exception occurred for the EF factor at the 14:00–15:00 interval on the partly cloudy days, with an R^2 of ~0.91.

4.4. Evaluation using satellite estimates

In the practical application of the four upscaling methods to the extrapolation of instantaneous ET estimates from remote sensing data, the accuracy of the extrapolated daily ET is controlled by the uncertainties from both the upscaling methods and the ET model. Using ground-based measurements alone, the analyses in Sections 4.2 and 4.3 comprehensively evaluated the four upscaling methods without considering the uncertainty in the instantaneous (half-hourly and hourly) ET estimates. In this section, we focus on the application of the four ET upscaling methods to the MODIS-derived instantaneous ET by the two-source N95 model at the 55 Terra overpass times and 46 Aqua overpass times, as described in Section 3.2. Our previous study showed that the RE correction method yields the best correspondence between the model-derived LE and the EC measurement at Yucheng station (Tang et al., 2012). Therefore, the RE correction method is used here to close the energy imbalance of the EC-measured LE for validation against the satellite-derived LE at both the instantaneous and daily scales.

Because the inaccurate atmospheric correction, emissivity correction and pixel shift or geolocation error are likely to underestimate/overestimate the MODIS temperature (Becker & Li, 1990; Wan & Li, 2008; Li et al., 2013a; Li et al., 2013b), the MODIS land surface temperature (LST) is first compared in Fig. 8a with the temperature estimated from the simultaneous tower-based upwelling and reflected downwelling longwave radiation measurements to determine whether there was any significant BIAS. A significant overestimation of MODIS LST and large scatter was found in the comparison at the Aqua overpass times with a positive BIAS (MODIS LST minus ground LST) of 2.1 K and an RMSE of 4.0 K. The MODIS LST at the Aqua overpass time on DOY (day of year) 126, 2010, significantly overestimated the ground LST by as much as 8.5 K due to the local irrigation. Better agreement was obtained at the Terra overpass times with a negative BIAS of −0.1 K and an RMSE of 2.9 K. The underestimation of MODIS LST could reach as high as 5.9 K at the Terra overpass time on DOY = 2009-120, perhaps because of the cirrus effect. Based on these results, to provide the most accurate inputs for driving the N95 model, corrections were made to the MODIS LST using the linear least square fit as shown in Fig. 8a. Moreover, if the difference (ground LST minus corrected MODIS LST) between ground LST and the corrected MODIS LST was larger than 1 K, the corrected MODIS LST would be replaced by the ground LST to eliminate the significant underestimation of LST caused by the linear least square fit for further analysis.

Fig. 8b compares the instantaneous surface net radiation (R_n) estimated from the N95 model using the corrected MODIS LST with ground measurements. It shows that the N95 model underestimated R_n at both the Terra and Aqua overpass times, with a negative BIAS within −22 W/m^2. The performance of the N95 model in estimating R_n was shown to be slightly better at the Terra overpass times (RMSE = 28 W/m^2) than at the Aqua overpass times (RMSE = 32 W/m^2), which may be partly relevant to the accuracy of the corrected MODIS LST. Because there were no multiple measurements of soil heat flux (G) to obtain a representative spatial sample, and because the heat storage above the plate was not accounted for, a comparison with the modeled G was not made.

Fig. 8c compares the instantaneous LE estimated from the N95 model using the corrected MODIS LST with the EC measurements corrected by the RE correction method. Due to the limited spatial representativeness of the measured G, the estimated G from the N95 model was used together with the R_n measurement to provide reliable pixel-averaged surface available energy for the correction of EC-measured LE. At the instantaneous time scale, it was evident that with the use of the corrected surface temperature a good agreement between the model-estimated LE and LE measurement was obtained at both the Terra and the Aqua overpass times, although a slight overestimation with a BIAS of 16 W/m^2 was found at the Terra overpass times. The RMSE and R^2 were 46 W/m^2 (13% of the observed mean) and 0.916, respectively, at the Terra overpass times and 34 W/m^2 (9% of the observed mean) and 0.948, respectively, at the Aqua overpass times. The difference in the model performance at the Terra and Aqua overpass times was associated with the use of the corrected MODIS temperature. Because of the relatively large scatter in the comparison of the low LE (<300 W/m^2), the performance of the N95 model at the Terra overpass times was shown to be slightly worse than that at the Aqua overpass times. The good performance of the N95 model demonstrated the necessity of making corrections to the MODIS LST and the N95 model was able to provide accurate remote sensing instantaneous LE for the upscaling methods.

Fig. 8d compares the daily ET extrapolated from the model-derived instantaneous LE using the four upscaling methods with the EC measurement corrected using the RE correction method. Because it was generally assumed that daily G could be negligible in applying the constant EF method in practical applications, we used daily R_n measurements rather than daily R_n–G measurements to upscale the remote sensing instantaneous ET for the EF upscaling method in this study, although some studies (Chávez et al., 2008) have recommended that the average daily G not be neglected. Table 1 shows the statistical measures of the performance of the four upscaling methods in extrapolating the instantaneous ET estimated

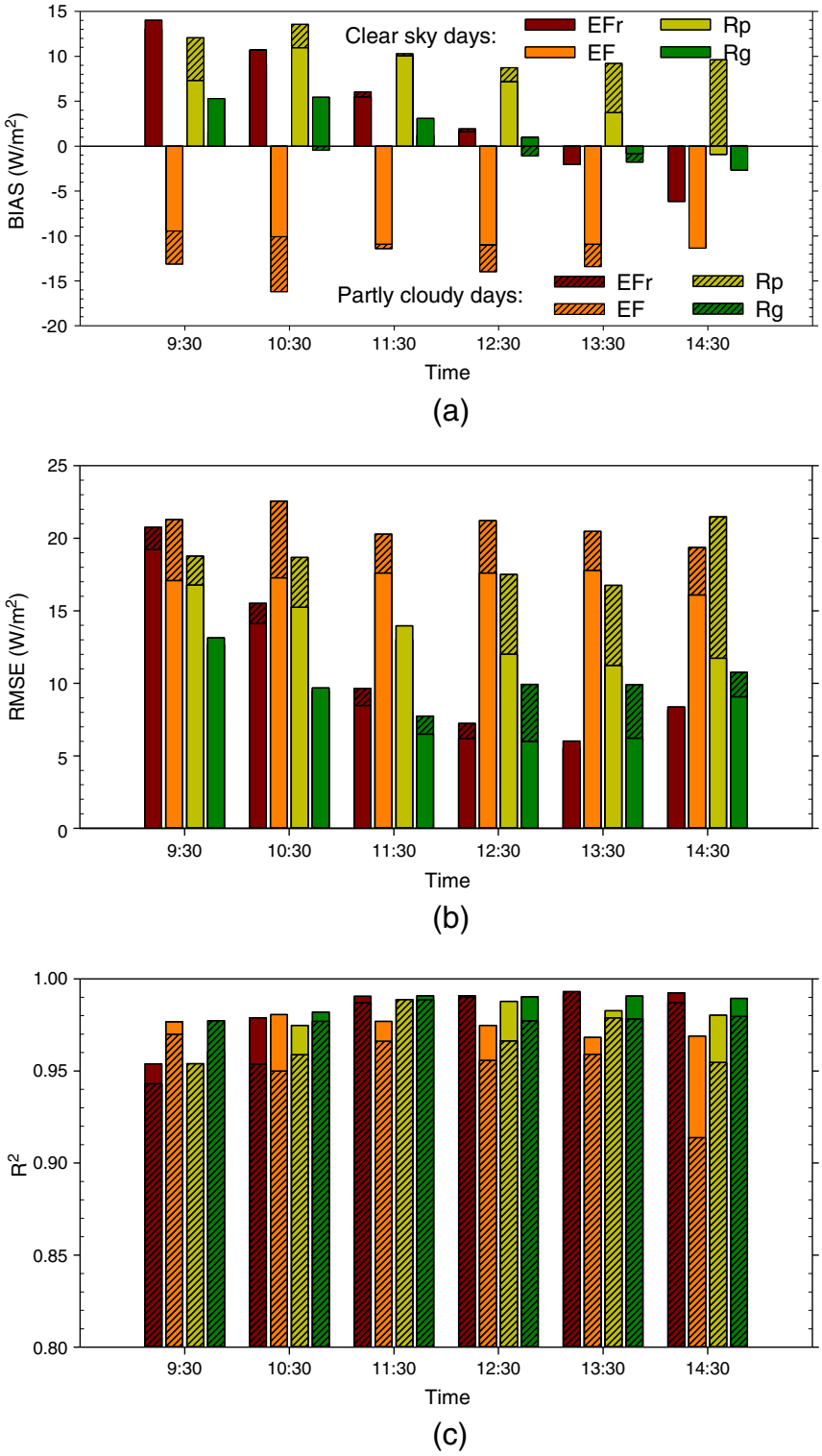

Fig. 7. Same as Fig. 4, but for the application of energy closure of the EC-measured LE using the residual energy correction method.

from the N95 model at the 101 satellite (55 MODIS/Terra and 46 MODIS/Aqua) overpass times. It can be seen that using the R_g factor gave the best performance, whereas using the R_p factor gave the worst performance in upscaling the remote sensing model-estimated LE. Using the EF factor underestimated the daily ET by 11%, while the remaining three factors overestimated the daily ET by a range of 5%–18%, which is consistent with the findings shown in Section 4.3 using the completely ground-based measurements. Using the EF_r factor gave the same magnitude of RMSE but a larger BIAS compared with using the R_g factor. Using the R_p factor gave a larger absolute BIAS and RMSE than using the EF factor, which may be due to the counteraction effect at the small magnitude of LE for the EF method.

4.5. Discussions

From mid-morning to mid-afternoon, the EF_r, R_p, and R_g factors were larger or smaller than or equal to their daily averages, while the EF factor was systematically smaller than its daily average on clear sky days, as

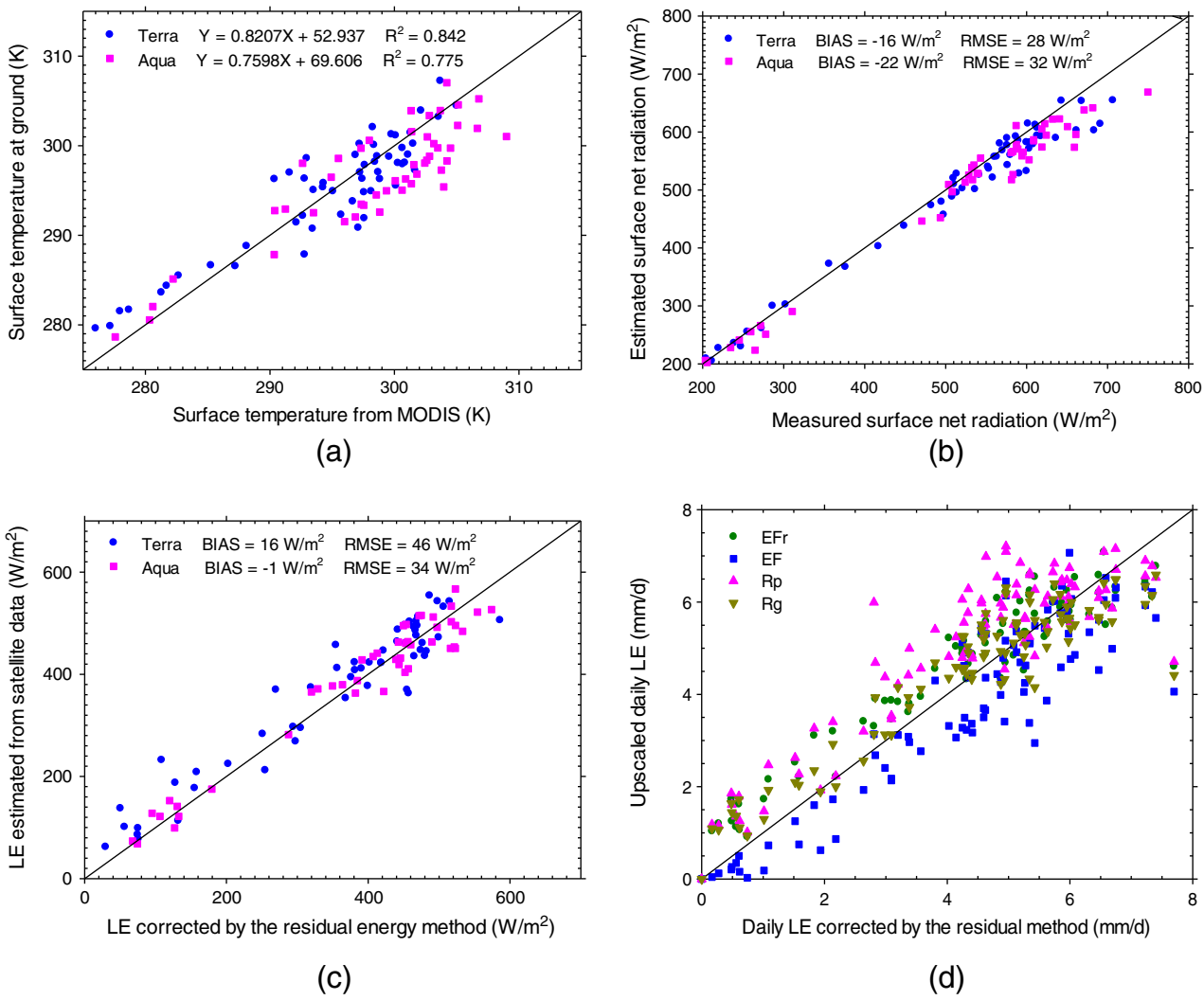

Fig. 8. (a) Comparison of land surface temperature (LST) derived from MODIS data with LST estimated from tower measurements of upwelling and reflected downwelling longwave radiation, (b) comparison of the instantaneous surface net radiation estimated from MODIS data using the N95 model with ground-based measurement, (c–d) comparison of the instantaneous latent heat flux estimated from MODIS data using the N95 model and the daily latent heat flux extrapolated from the model-derived ET using the four upscaling methods with eddy covariance system measurements corrected by the residual energy method.

shown in Fig. 2. With the presence of clouds during daytime on a partly cloudy day, because global solar radiation and surface net radiation decrease more seriously than latent heat flux (Crago, 1996; Van Niel et al., 2012, 2011), the EF, R_g, and EF_r will increase, causing their respective daily averages to increase. However, because the extraterrestrial solar radiation is not affected by clouds, the R_p at a given clear sky time will decrease if it becomes cloudy, causing the daily average to decrease. The magnitude of the increase or decrease of the daily averages of the four upscaling factors depends on the cloud amount and duration.

If using the EF, R_g, and EF_r factors to upscale LE underestimates the daily value on a clear sky day for a given time interval, the relative underestimation of daily LE will become more serious for all three factors on a partly cloudy day because the difference between these factors at the clear sky time and their daily averages is increased. If using the R_g and EF_r factors to upscale LE overestimates the daily value on a clear sky day for a given time interval, the relative overestimation of daily LE will be weakened on a partly cloudy day. In contrast, if using the R_p factor to upscale LE underestimates (overestimates) the daily value on a clear sky day for a given time interval, the relative underestimation (overestimation) of daily LE will be weakened (more serious) on a partly cloudy day because the difference between the R_p factor at the clear sky time and their daily averages is decreased. These interpretations are consistent with the results obtained in Section 4.2.

The EF upscaling method is shown to systematically underestimate the daily LE from mid-morning to mid-afternoon for both clear sky days and partly cloudy days before and after the energy imbalance of the EC measurement is closed. This underestimation is perhaps due to the concave-up shape of the EF during daytime with no account of the

Table 1
Statistical measures of the performance of four representative upscaling methods in converting the instantaneous ET estimated from the N95 model at the 101 satellite (55 MODIS/Terra and 46 MODIS/Aqua) overpass times between late April 2009 and late October 2011, with the EC measurements corrected by the residual energy method (R_BIAS = BIAS/$\overline{O}$*100%, R_RMSE = RMSE/$\overline{O}$*100%, where $\overline{O}$ represents the average of the EC-measured daily latent heat flux).

	$\overline{O}$ (mm)	EF_r	EF	R_p	R_g
BIAS (mm/d)		0.4	−0.5	0.7	0.2
RMSE (mm/d)		0.8	0.9	1.1	0.8
R^2		0.902	0.871	0.851	0.905
Slope	4.1	0.78	0.84	0.79	0.78
Intercept (mm/d)		1.3	0.1	1.6	1.1
R_BIAS (%)		9	−11	18	5
R_RMSE (%)		19	22	27	19

nighttime ET (accounting for ~8% on average of daily totals in this study). Hoedjes et al. (2008) have shown that EF remains conservative during daytime under dry conditions but exhibits a concave-up shape under wet conditions. Moreover, the EF can exhibit a flat shape or a parabolic shape that is different from the concave-up shape (Gentine et al., 2011). The underestimation of daily LE from the EF upscaling method has also been reported by a great number of papers (Gentine et al., 2007, 2011; Hoedjes et al., 2008; Delogu et al., 2012; Ryu et al., 2012; Van Niel et al., 2012). The tendency of the BIAS and RMSE to decrease from mid-morning to mid-afternoon has also been found in previous studies (Brutsaert & Sugita, 1992; Ryu et al., 2012). The presence of clouds further deteriorates the performance of the EF upscaling method on clear sky days.

Just as the assumption of daytime conservation of EF implies, use of the constant EF method should have been made on the estimates of daytime LE rather than daily (24-h) LE because the nighttime EF has different temporal characteristics from the daytime counterpart. However, because models for estimating daytime averaged surface available energy generally do not exist (most models are developed for the daily (24-h) estimates) and because the daily LE has real values in practical application, it is necessary to extrapolate the instantaneous LE to the daily scale using the 24-h averaged available energy (Gómez et al., 2005; Chávez et al., 2008; Van Niel et al., 2011). Past studies have estimated daily LE by either making corrections to the daytime LE upscaled from the constant EF method (Brutsaert & Sugita, 1992) or directly applying the constant EF method to a daily scale (Gómez et al., 2005). Using the latter approach to estimate daily LE is likely to be error-prone and, at most times, will underestimate the daily LE as shown in this study because the relatively conservative EF near midday, sometimes approximating the daytime average, cannot be representative of its daily value unless the nighttime LE accounts for a negligible fraction of daily totals.

Similar to the constant EF method, it seems that the modeled R_p and observed R_g methods are more suitable for the upscaling of instantaneous LE to daytime values, as the nighttime extraterrestrial solar radiation and observed global solar radiation equal zero and make no contribution to the nighttime and daily LEs. It is expected that the observed R_g method can outperform the modeled R_p method during the partly cloudy days because, unlike with the observed global solar radiation, the presence of clouds does not have any influence on the extraterrestrial solar radiation and the effect of clouds is not reflected in the R_p factor at the clear sky satellite overpass time. However, this expectation can only be realized from noon to mid-afternoon in this study. This may be because in the mid-morning on clear sky days both factors underestimate their daily averages and the R_g factor has a relatively larger absolute BIAS than the R_p factor compared with their respective daily averages, as shown in Fig. 2b. If the R_p method tends to underestimate (overestimate) the daily LE on the clear sky days, it may perform better (even worse) due to the counteraction effect on the partly cloudy days, as interpreted previously.

Using the modeled R_p method and the observed R_g method is shown to first give an underestimation and then an overestimation of daily LE from mid-morning to mid-afternoon on both clear sky and partly cloudy days before the energy imbalance is closed, as shown in Figs. 2 and 4. After closing the energy imbalance from the BR and RE correction methods, the R_p method overall systematically overestimates the daily LE. Similar to the results without the energy imbalance correction, the R_g method undergoes first an underestimation and then an overestimation of the daily LE using the BR correction method. If the RE correction is made, first an overestimation and then an underestimation of the daily LE is found. The relatively better performance of the R_p and R_g methods than that of the EF method in this study has also been found in the work of Ryu et al. (2012) and Van Niel et al. (2012). Inconsistent results are obtained for the R_p and R_g methods from mid-morning to mid-afternoon. In the mid-morning, using the R_p method gives a lower absolute BIAS and RMSE than using the R_g method, whereas from noon to mid-afternoon opposite results are obtained. Moreover, the complementary relationship between the BIAS of the observed R_g method and that of the modeled R_p method found by Van Niel et al. (2012) can only be recognized near noontime.

The EF_r method can incorporate the effect of clouds on the observed global solar radiation during daytime and the variation of meteorological variables during both daytime and nighttime (Allen et al., 2007). It is expected that this method can theoretically produce good estimates of daily LE, as has been verified in this study from the lowest BIAS and RMSE in the four upscaling methods from mid-morning to mid-afternoon on both clear sky and partly cloudy days before energy imbalance correction. The BR and RE correction methods cause the daily LE to be overestimated during the morning and underestimated during the mid-afternoon for the EF_r method.

When the four upscaling factors are applied to upscale the remote sensing instantaneous LE in practical applications, mixed clear sky and partly cloudy days may be involved. Meanwhile, the accuracy of the upscaled daily ET will be co-determined by both the accuracy of the upscaling method and the accuracy of the instantaneous model-estimated LE. It is expected that the R_g and EF_r factors will have a better performance in upscaling the instantaneous LE estimated from the N95 model than the EF and the R_p factors if the remote sensing instantaneous LE estimates are insignificantly biased, as shown in Section 4.4. The R_p factor is shown to underperform the EF factor in upscaling the remote sensing LE in this study, which is inconsistent with the findings by Ryu et al. (2012) and the results obtained in Section 4.3 using completely ground-based measurements. Both Colaizzi et al. (2006) and Chávez et al. (2008) have shown, using data on clear sky days, that the EF_r method performs best for transpiring crops under advective and homogeneous surface conditions; however, for bare soil or other surfaces having a lower daily ET, the EF method has a better agreement with the daily LE, which is contradictory to our findings. Our results suggest that even when the daily ET is relatively low, the EF_r method still outperforms the EF method, as shown in Section 4.3. Chávez et al. (2008) partly attributed the worse performance of the EF_r method to the spatially unrepresentative weather station measurements, but we think it may be caused by the uncertainty in the estimation of the remote sensing instantaneous LE in their study. Note that the significantly biased estimation of the remote sensing instantaneous LE (for example, the instantaneous LE will be significantly overestimated by the N95 model if the MODIS temperature is not corrected) may confound the performances of the four upscaling methods. The underestimation of the EF factor may be counteracted by the overestimation of the instantaneous LE, producing an unbiased upscaled daily LE.

The relative RMSE (RMSE divided by the observed mean) in the comparison of the remote sensing instantaneous LE (9%–13%) is shown to be increased when the upscaled daily ET is compared (19%–27%). To determine whether the RMSE could be reduced over a longer time scale, we made a further attempt to upscale the remote sensing instantaneous LE to an eight-day average. A comparison of the upscaled 12 eight-day and 1 five-day averaged ET over the selected 101 MODIS overpass times with the EC measurements shows that the RMSE is significantly reduced for all four upscaling factors compared with that at the daily scale, which is consistent with the findings by Ryu et al. (2012). The relative RMSE is 13% for the EF_r and EF factors, 20% for the R_p factor, and 9% for the R_g factor. It seems that with the increasing integration period, the EF factor could have an RMSE magnitude similar to the EF_r factor.

Same as reported in previous studies (Colaizzi et al., 2006; Gentine et al., 2007, 2011; Delogu et al., 2012), this study also shows that near noon has the optimal correspondence for the satellite overpass to upscale instantaneous LE for the EF_r, R_p, and R_g factors.

5. Summary and conclusions

Because ET estimates at daily or longer time scales are of more significance and appeal more strongly to the water resources manager than

instantaneous ET estimates, this study evaluated four representative temporal upscaling schemes using long-term ground-based measurements and MODIS estimates from late April 2009 to late October 2011 at the Yucheng station. The final goal of this study was to provide scientific guidance for our development of an operational and more accurate ET-upscaling method with easy data access in the future.

Overall, all four upscaling factors showed better agreement with the daily averages from noon to mid-afternoon. The EF method had the worst performance among the four upscaling methods and underestimated the daily ET estimates on both the clear sky and partly cloudy days before and after the energy imbalance correction. Before the energy imbalance was corrected, the EF_r method performed best in the upscaling of instantaneous LE on both clear sky and partly cloudy days. The R_p (R_g) method performed the second (third) best in the mid-morning and the third (second) best from noon to mid-afternoon. After the BR and the RE correction methods, the best-performing EF_r method was shown to have the second-lowest absolute BIAS (higher than the R_g method) from mid-morning to mid-afternoon. From mid-morning to noon, the R_g (EF_r) method had the lowest (second-lowest) RMSE, whereas from noon to mid-afternoon, the EF_r (R_g) method had the lowest (second-lowest) RMSE. The presence of clouds could either increase or decrease the BIAS, but it generally increased the RMSE for the all four upscaling methods.

If the four upscaling schemes were applied to convert the instantaneous remote sensing estimates of ET to daily values, the performance was further controlled by the accuracy of the remote sensing ET estimates. A significantly biased estimation of remote sensing instantaneous LE may confound the performances of the four upscaling methods. With the insignificantly biased estimates of the instantaneous LE from the N95 model, using the EF factor underestimated the daily ET by 11%, while the remaining three factors overestimated the daily ET by a range of 5%–18%. The relative RMSE was shown to increase and the R^2 to decrease when the comparison of the remote sensing instantaneous LE was changed to that of the upscaled daily ET, most likely indicating that the random errors could not be significantly removed in the daily ET upscaling. However, the scatter was significantly reduced for all four upscaling methods when extrapolating the remote sensing instantaneous LE to a longer time period (e.g., eight days).

One of the main limitations of the R_p, the R_g, and the EF methods is that the influence of the horizontal advection and the variation of meteorological variables (e.g., wind speed, vapor pressure deficit) cannot be effectively incorporated because the R_p method is controlled only by the Sun–Earth geometry for a given day at a given site and because the daily global solar radiation and available energy are less dependent (if not independent) on these meteorological variables. The EF_r method using the ET for a reference crop estimated from the Penman–Monteith equation can incorporate the variations of the meteorological variables and the horizontal advection. When intensive ground-based measurements of meteorological variables (e.g., global solar radiation, air temperature, wind speed, and relative humidity) are readily available, it is recommended that the EF_r method be used for LE upscaling. Otherwise, the R_g method (if observed global solar radiation is available) and the R_p method are recommended, in order. The merit of the R_p method lies in its independence from ground-based measurements.

To accurately extrapolate the instantaneous remote sensing estimates of ET, it is essential to find a conservative upscaling factor that can be independent of the variation in the atmospheric variables and can, in addition, incorporate the horizontal advection. Of the four upscaling schemes, the EF_r method was shown to perform well in capturing the variation in the diurnal LE. The weakness of this approach lies in the requirement for detailed input data on atmospheric variables, e.g., the air temperature, relative humidity, global solar radiation, and wind speed in half-hourly or hourly time steps. These instantaneous and daily data may not be available due to the limited ground networks established for data collection on the Earth, especially in remote areas. A potential improvement to the EF_r method would be to introduce a variable canopy resistance for the reference grass instead of using the fixed value (Todorovic, 1999). One possible solution to the lack of available atmospheric inputs for the reference ET estimation in deriving daily ET would be to combine the MODIS instrument with daily weather forecast information. MOD07 and MYD07 freely provide the profiles of instantaneous dew points and air temperatures at different levels, and the necessary maximum and minimum daily air temperatures, wind scale, and cloud conditions are given in the daily weather forecast information. In future work, we will examine the feasibility of upscaling the instantaneous ET estimated from the remote sensing model to daily and longer time scales using the EF_r method with a variable canopy resistance and the synergy between the MOD07 (MYD07) profile and weather forecast information.

Acknowledgments

We thank the hard-working staff members at the Yucheng Comprehensive Experimental Station who are responsible for the setup and maintenance of the ground-based instruments and data collection. We also thank Associate Professor Yuanyuan Jia and Professor Chuanrong Li in the Academy of Opto-Electronics, Chinese Academy of Sciences, who cooperatively provided the surface measurements used in this study. This work was partly supported by the National Natural Science Foundation of China under grant 41201366 and 41101332 and by the China Postdoctoral Science Foundation funded project under grant 07Z7602MZ1.

References

Allen, R. G., Pereira, L. S., Raes, D., Raes, D., & Smith, M. (1998). *Crop evapotranspiration: Guidelines for computing crop water requirement. Irrigation and Drainage Paper 56*Rome, Italy: FAO.

Allen, R. G., Pruitt, W. O., Wright, J. L., Howell, T. A., Ventura, F., Snyder, R., et al. (2006). A recommendation on standardized surface resistance for hourly calculation of reference ETo by the FAO56 Penman–Monteith method. *Agricultural Water Management*, *81*, 1–22.

Allen, R. G., Tasumi, M., & Trezza, R. (2007). Satellite-based energy balance for mapping evapotranspiration with internalized calibration (METRIC)-model. *Journal of Irrigation and Drainage Engineering*, *133*(4), 380–394.

Anderson, M. C., Norman, J. M., Kustas, W. P., Houborg, R., Starks, P. J., & Agam, N. (2008). A thermal-based remote sensing technique for routine mapping of land-surface carbon, water and energy fluxes from field to regional scales. *Remote Sensing of Environment*, *112*, 4227–4241.

ASCE-EWRI (2005). The ASCE standardized reference evapotranspiration equation. *Technical committee report to the environmental and water resources Institute of the American Society of Civil Engineers from the Task Committee on Standardization of Reference Evapotranspiration.* 1801 Alexander Bell Drive, Reston, VA 20191-4400: ASCE-EWRI (173 pp.).

Baldocchi, D., Falge, E., Gu, L., Olson, R., Hollinger, D., Running, S., et al. (2001). FLUXNET: A new tool to study the temporal and spatial variability of ecosystem-scale carbon dioxide, water vapor, and energy flux densities. *Bulletin of the American Meteorological Society*, *11*, 2415–2434.

Becker, F., & Li, Z. -L. (1990). Towards a local split window method over land surfaces. *International Journal of Remote Sensing*, *11*(3), 369–393.

Brutsaert, W., & Sugita, M. (1992). Application of self-preservation in the diurnal evolution of the surface energy budget to determine daily evaporation. *Journal of Geophysical Research*, *97*, 18377–18382.

Burba, G., & Anderson, D. (2010). *A brief practical guide to eddy covariance flux measurements: Principles and workflow examples for scientific and industrial applications.* Lincoln, Nebraska, USA: LI-COR Biosciences (212 pp.).

Cammalleri, C., Anderson, M. C., Ciraolo, G., D'Urso, G., Kustas, W. P., La Loggia, G., et al. (2012). Applications of a remote sensing-based two-source energy balance algorithm for mapping surface fluxes without in situ air temperature observations. *Remote Sensing of Environment*, *124*, 502–515.

Chávez, J. L., Neale, C. M., Prueger, J. H., & Kustas, W. P. (2008). Daily evapotranspiration estimates from extrapolating instantaneous airborne remote sensing ET values. *Irrigation Science*, *27*, 67–81.

Choi, M., Kustas, W. P., Anderson, M. C., Allen, R. G., Li, F., & Kjaersgaard, J. H. (2009). An intercomparison of three remote sensing-based surface energy balance algorithms over a corn and soybean production region (Iowa, U.S.) during SMACEX. *Agricultural and Forest Meteorology*, *149*, 2082–2097.

Colaizzi, P. D., Evett, S. R., Howell, T. A., & Tolk, J. A. (2006). Comparison of five models to scale daily evapotranspiration from one-time-of-day measurements. *Transactions of ASAE*, *49*, 1409–1417.

Crago, R. (1996). Conservation and variability of the evaporative fraction during the daytime. *Journal of Hydrology*, *180*, 173–194.

Delogu, E., Boulet, G., Olioso, A., Coudert, B., Chirouze, J., Ceschia, E., et al. (2012). Reconstruction of temporal variations of evapotranspiration using instantaneous estimates at the time of satellite overpass. *Hydrology and Earth System Sciences*, *16*, 2995–3010.

Foken, T. (2008). The energy balance closure problem: An overview. *Ecological Applications*, *18*, 1351–1367.

Galleguillos, M., Jacob, F., Prévot, L., Lagacherie, P., & Liang, S. (2011). Mapping daily evapotranspiration over a Mediterranean vineyard watershed. *IEEE Geoscience and Remote Sensing Letters*, *8*(1), 168–172.

Gentine, P., Entekhabi, D., Chehbouni, A., Boulet, G., & Duchemin, B. (2007). Analysis of evaporative fraction diurnal behavior. *Agricultural and Forest Meteorology*, *143*(1–2), 13–29.

Gentine, P., Entekhabi, D., & Polcher, J. (2011). The diurnal behavior of evaporative fraction in the soil–vegetation–atmospheric boundary layer continuum. *Journal of Hydrometeorology*, *12*, 1530–1546.

Gómez, M., Olioso, A., Sobrino, J., & Jacob, F. (2005). Retrieval of evapotranspiration over the Alpilles/ReSeDA experimental site using airborne POLDER sensor and a thermal camera. *Remote Sensing of Environment*, *96*(3/4), 399–408.

Hall, F. G., Huemmrich, K. F., Goetz, S. J., Sellers, P. J., & Nickerson, J. E. (1992). Satellite remote sensing of surface energy balance: Success, failures and unresolved issues in FIFE. *Journal of Geophysical Research*, *97*, 19061–19089.

Hoedjes, J. C. B., Chehbouni, A., Jacob, F., Ezzahar, J., & Boulet, G. (2008). Deriving daily evapotranspiration from remotely sensed instantaneous evaporative fraction over olive orchard in semi-arid Morocco. *Journal of Hydrology*, *354*, 53–64.

Jackson, R. D., Hatfield, J. L., Reginato, R. J., Idso, S. B., & Pinter, P. (1983). Estimation of daily evapotranspiration from one time of day measurements. *Agricultural Water Management*, *7*, 351–362.

Kalma, J.D., McVicar, T. R., & McCabe, M. F. (2008). Estimating land surface evaporation: A review of methods using remotely sensed surface temperature data. *Surveys in Geophysics*, *29*, 421–469.

Kustas, W. P., & Norman, J. M. (1997). A two-source approach for estimating turbulent fluxes using multiple angle thermal infrared observations. *Water Resources Research*, *33*, 1495–1508.

Kustas, W. P., & Norman, J. M. (2000). A two-source energy balance approach using directional radiometric temperature observations for sparse canopy covered surfaces. *Agronomy Journal*, *92*, 847–854.

Lhomme, J. -P., & Elguero, E. (1999). Examination of evaporative fraction diurnal behavior using a soil-vegetation model coupled with a mixed-layer model. *Hydrology and Earth System Sciences*, *3*(2), 259–270.

Li, F. Q., Kustas, W. P., Anderson, M. C., Prueger, J. H., & Scott, R. L. (2008). Effect of remote sensing spatial resolution on interpreting tower-based flux observations. *Remote Sensing of Environment*, *112*, 337–349.

Li, Z. -L., Stoll, M. -P., Zhang, R., Jia, L., & Su, Z. (2001). On the separate retrieval of soil and vegetation temperatures from ATSR data. *Science in China (Series D)*, *44*, 97–111.

Li, Z. -L., Tang, R. L., Wan, Z., Bi, Y., Zhou, C., Tang, B., et al. (2009). A review of current methodologies for regional evapotranspiration estimation from remotely sensed data. *Sensors*, *9*, 3801–3853.

Li, Z. -L., Tang, B. H., Wu, H., Ren, H., Yan, G., Wan, Z., et al. (2013a). Satellite-derived land surface temperature: Current status and perspectives. *Remote Sensing of Environment*, *131*, 14–37.

Li, Z. -L., Wu, H., Wang, N., Shi, Q., Sobrino, J. A., Wan, Z., et al. (2013b). Land surface emissivity retrieval from satellite data. *International Journal of Remote Sensing*, *34*(9–10), 3084–3127.

Li, Z. -L., Zhang, R., Sun, X., Su, H., Tang, X., Zhu, Z. J., et al. (2004). Experimental system for the study of the directional thermal emission of natural surfaces. *International Journal of Remote Sensing*, *25*, 195–204.

Monteith, J. L. (1965). Evaporation and environment. *Symposia of the Society for Experimental Biology*, *19*, 205–234.

Nichols, W. E., & Cuenca, R. H. (1993). Evaluation of the evaporative fraction for parameterization of the surface energy-balance. *Water Resources Research*, *29*(11), 3681–3690.

Norman, J. M., Kustas, W. P., & Humes, K. S. (1995). A two-source approach for estimating soil and vegetation energy fluxes from observations of directional radiometric surface temperature. *Agricultural and Forest Meteorology*, *77*, 263–293.

Ryu, Y., Baldocchi, D.D., Black, T. A., Detto, M., Law, B. E., Leuning, R., et al. (2012). On the temporal upscaling of evapotranspiration from instantaneous remote sensing measurements to 8-day mean daily-sums. *Agricultural and Forest Meteorology*, *152*, 212–222.

Sánchez, J. M., Kustas, W. P., Caselles, V., & Anderson, M. C. (2008). Modelling surface energy fluxes over maize using a two-source patch model and radiometric soil and canopy temperature observations. *Remote Sensing of Environment*, *112*, 1130–1143.

Shuttleworth, W. J., Gurney, R. J., Hsu, A. Y., & Ormsby, J. P. (1989). FIFE: The variation in energy partition at surface flux sites. *International Association of Hydrological Sciences Publication*, *186*, 67–74.

Sobrino, J. A., Gómez, M., Jiménez-Muñoz, J. C., & Olioso, A. (2007). Application of a simple algorithm to estimate the daily evapotranspiration from NOAA-AVHRR images for the Iberian Peninsula. *Remote Sensing of Environment*, *110*, 139–148.

Stoy, P. C., Mauder, M., Foken, T., Marcolla, B., Boegh, E., Ibrom, A., et al. (2013). A data-driven analysis of energy balance closure across FLUXNET research sites: The role of landscape scale heterogeneity. *Agricultural and Forest Meteorology*, *171*, 137–152.

Tang, R. L., Li, Z. -L., Jia, Y., Li, C., Chen, K. -S., Sun, X., et al. (2012). Evaluating one- and two-source energy balance models in estimating surface evapotranspiration from Landsat-derived surface temperature and field measurements. *International Journal of Remote Sensing*, http://dx.doi.org/10.1080/01431161.2012.716529.

Tang, R. L., Li, Z. -L., Jia, Y., Li, C., Sun, X., Kustas, W. P., et al. (2011). An intercomparison of three remote sensing-based energy balance models using Large Aperture Scintillometer measurements over a wheat–corn production region. *Remote Sensing of Environment*, *115*, 3187–3202.

Tang, R. L., Li, Z. -L., Chen, K. -S., Jia, Y., Li, C., & Sun, X. (2013). Spatial-scale effect on the SEBAL model for evapotranspiration estimation using remote sensing data. *Agricultural and Forest Meteorology*, *174*, 28–42.

Todorovic, M. (1999). Single-layer evapotranspiration model with variable canopy resistance. *Journal of Irrigation and Drainage Engineering*, *125*(5), 235–245.

Trezza, R. (2002). *Evapotranspiration using a satellite-based surface energy balance with standardized ground control.* (Ph.D. dissertation, USU, Logan, UT, 339 pp.).

Twine, T. E., Kustas, W. P., Norman, J. M., Cook, D. R., Houser, P. R., Meyers, T. P., et al. (2000). Correcting eddy-covariance flux underestimates over a grassland. *Agricultural and Forest Meteorology*, *103*, 279–300.

Van Niel, T. G., McVicar, T. R., Roderick, M. L., Van Dijk, A. I., Beringer, J., Hutley, L., et al. (2012). Upscaling latent heat flux for thermal remote sensing studies: Comparison of alternative approaches and correction of bias. *Journal of Hydrology*, *468–469*, 35–46.

Van Niel, T. G., McVicar, T. R., Roderick, M. L., Van Dijk, A. I., Renzullo, L. J., & Van Gorsel, E. (2011). Correcting for systematic error in satellite-derived latent heat flux due to assumptions in temporal scaling: Assessment from flux tower observations. *Journal of Hydrology*, *409*, 140–148.

Wan, Z., & Dozier, J. (1996). A generalized split-window algorithm for retrieving land-surface temperature from space. *IEEE Transactions on Geoscience and Remote Sensing*, *34*, 892–905.

Wan, Z., & Li, Z. -L. (2008). Radiance-based validation of the V5 MODIS land-surface temperature product. *International Journal of Remote Sensing*, *29*(17), 5373–5395.

Webb, E. K., Pearman, G. I., & Leuning, R. (1980). Correction of flux measurements for density effects due to heat and water vapour transfer. *Quarterly Journal of the Royal Meteorological Society*, *106*(447), 85–100.

Wilson, K., Goldstein, A., Falge, E., Aubinet, M., Baldocchi, D., Berbigier, P., et al. (2002). Energy balance closure at FLUXNET sites. *Agricultural and Forest Meteorology*, *113*, 223–243.

Wu, H., & Li, Z. -L. (2009). Scale issues in remote sensing: A review on analysis, processing and modeling. *Sensors*, *9*, 1768–1793.